

Superconducting Nanowire Single-Photon Detectors



K. K. Berggren

*Department of Electrical Engineering and Computer Science, Massachusetts Institute of Technology,
Cambridge, Massachusetts 02139, USA*

11114-rochester

berggren@mit.edu

1

I'm going to present work today from the quantum nanofabrication group at MIT done in collaboration with MIT Lincoln Lab and NIST. I will be focusing on ultranarrow Superconductive Single-Photon detectors.

KEYWORDS: title, utility, rle logo



Image from messenger spacecraft, downloaded from website indicated, as well as list of instrumentation on the spacecraft.

15 MB/day is average

Two records, 1 Gb each

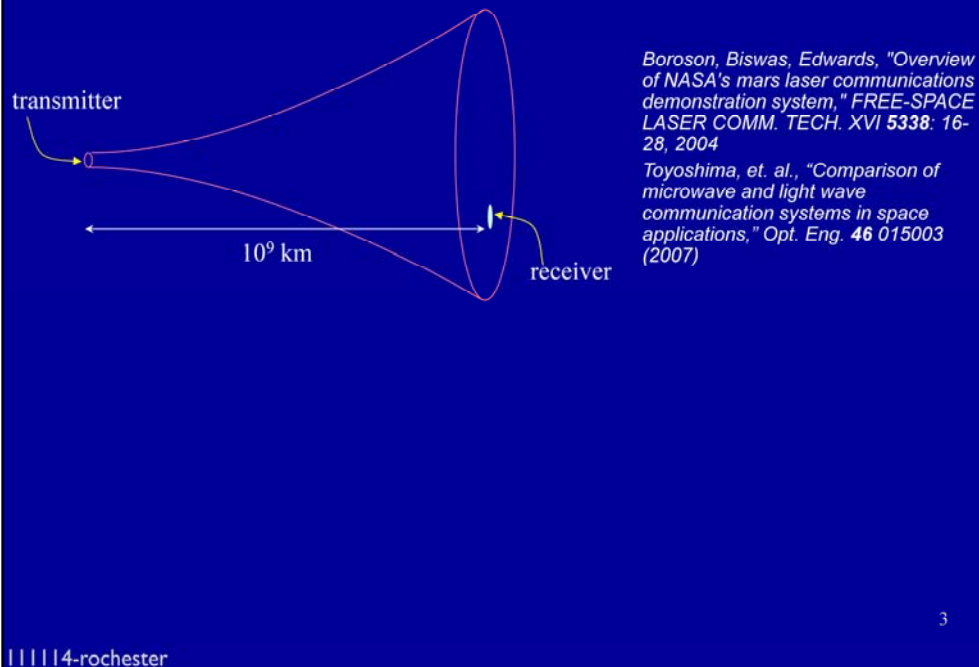
Data rate ranges from 10 bits/sec to 100 kBit/sec

Two high-resolution digital cameras

Gamma ray, neutron, x-ray spectrometers

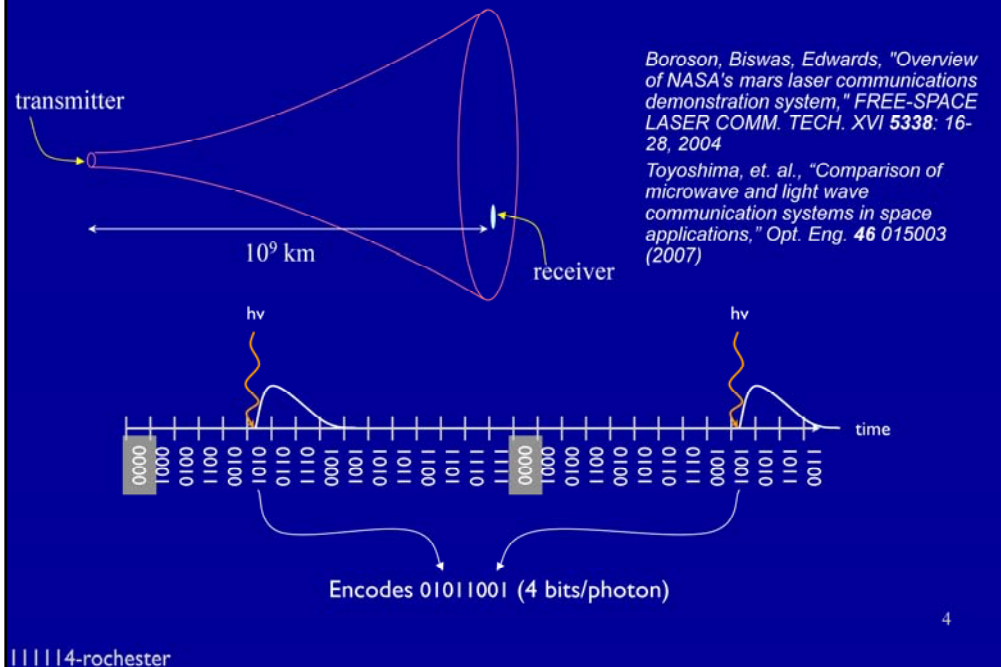
magnetometer

Free-Space Optical Communications



Here we review a paper by Boroson et al., in which the basic design issues of a mars to earth free-space optical link are described, including the encoding scheme.

Free-Space Optical Communications



Here we review a paper by Boroson et al., in which the basic design issues of a mars to earth free-space optical link are described, including the encoding scheme.

Photons

- Illumination in eye from 1 pixel of laptop at 100 km in 1 sec
- Energy inversely proportional to wavelength
 - Longer wavelength => harder to detect

11114-rochester

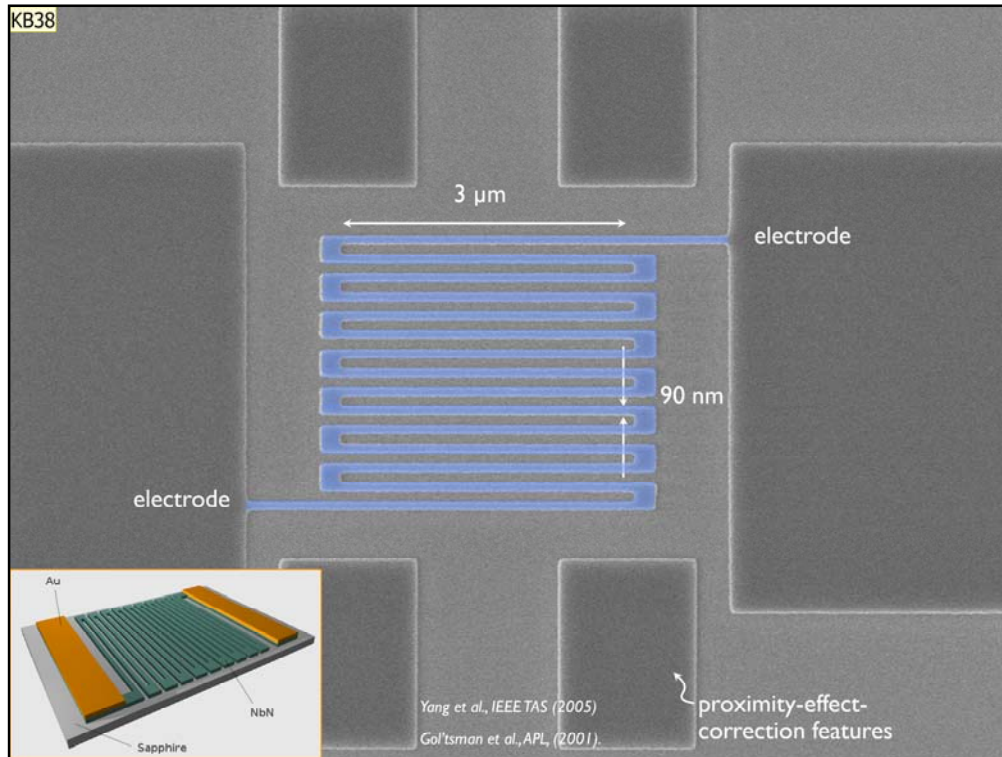
5

Berggren

This slide is intended to familiarize the audience with the challenge of the project, and to emphasize that detection of photons in the infrared ($\sim 1.5 \mu\text{m}$) is much more challenging than it is in the visible ($< 1 \mu\text{m}$) because of the lower photon energy, and the fact that the energy of the photon is less than the silicon bandgap, so that silicon detectors cannot be used in that range.

KEYWORDS: text, background

TITLE: Photons



This is a typical layout for an SNSPD detector. It is important to maximize the area of overlap of the detector with the optical beam (without reducing the nanowire width). We accomplish this by winding the wire into a boustrophedonic (or “meander”) pattern as shown in this SEM. You still lose a fair amount of the light through the gaps between the wires, but a lot less than you would lose with just a single wire. You also gain a lot by reducing those gaps, which is something we’re working on. The loss through the gaps isn’t quite proportional as you might expect, because the structures are subwavelength.

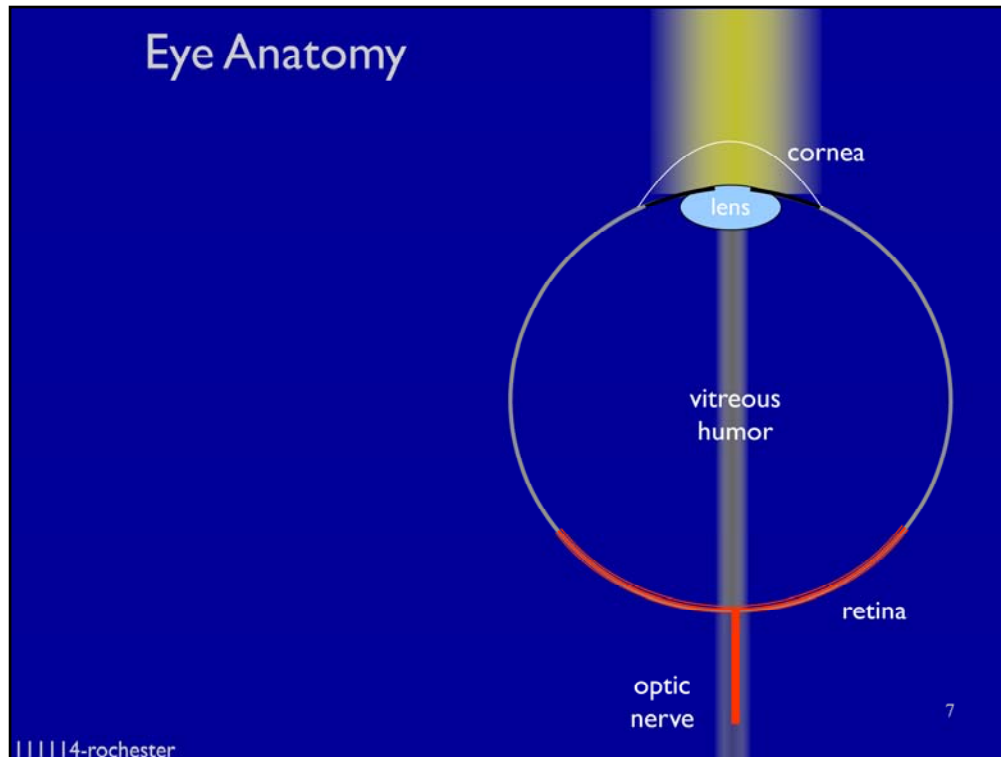
A lot of light is still lost due to reflection and transmission, however, so we added some optical enhancements to the device.

KEYWORDS: SNSPD, photodetector, micrograph, SEM

TITLE: SEM of “standard” SNSPD

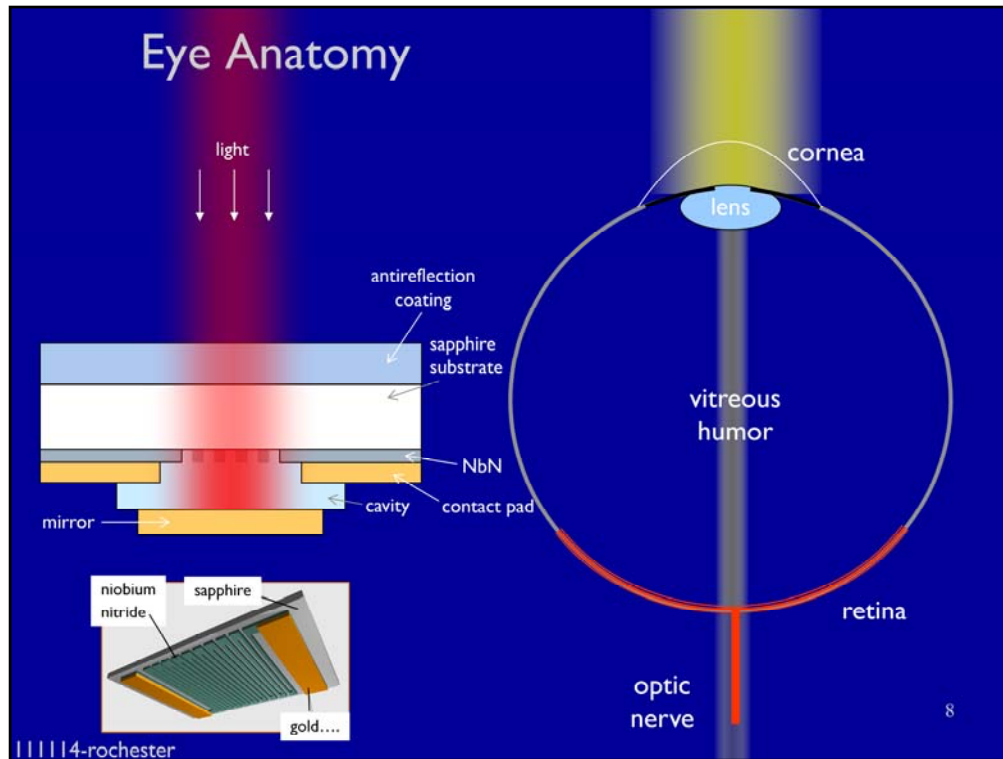
Slide 6

KB38 insert more about nanofab
Karl Berggren, 9/15/2008



Surprisingly, the human eye is a very good model for understanding the issues involved with low-level light detection.

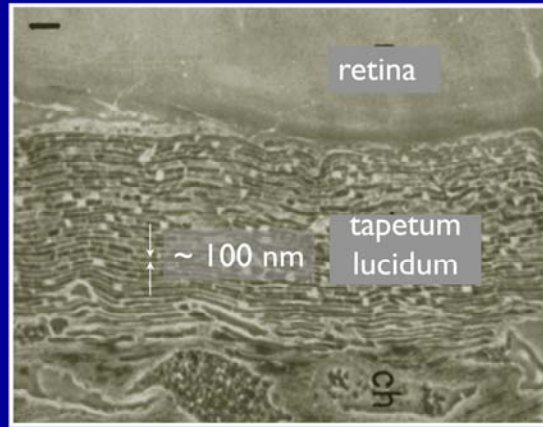
The rods are the primary sensors for low light levels (the cones are responsible for color sensing). Rods can easily detect single photons, but to avoid shot noise, multiple rods must fire for the brain to interpret it as a signal. While ~ 300 photons illuminate the eye, reflection from the cornea, absorption in the eye, and transmission through the eye account for a huge total amount of loss ($> 90\%$). The result is that only a few photons are required to detect the fully dark-adapted eye.



Surprisingly, the human eye is a very good model for understanding the issues involved with low-level light detection.

The rods are the primary sensors for low light levels (the cones are responsible for color sensing). Rods can easily detect single photons, but to avoid shot noise, multiple rods must fire for the brain to interpret it as a signal. While ~ 300 photons illuminate the eye, reflection from the cornea, absorption in the eye, and transmission through the eye account for a huge total amount of loss ($> 90\%$). The result is that only a few photons are required to detect the fully dark-adapted eye.

Tapetum Lucidum of a Cat



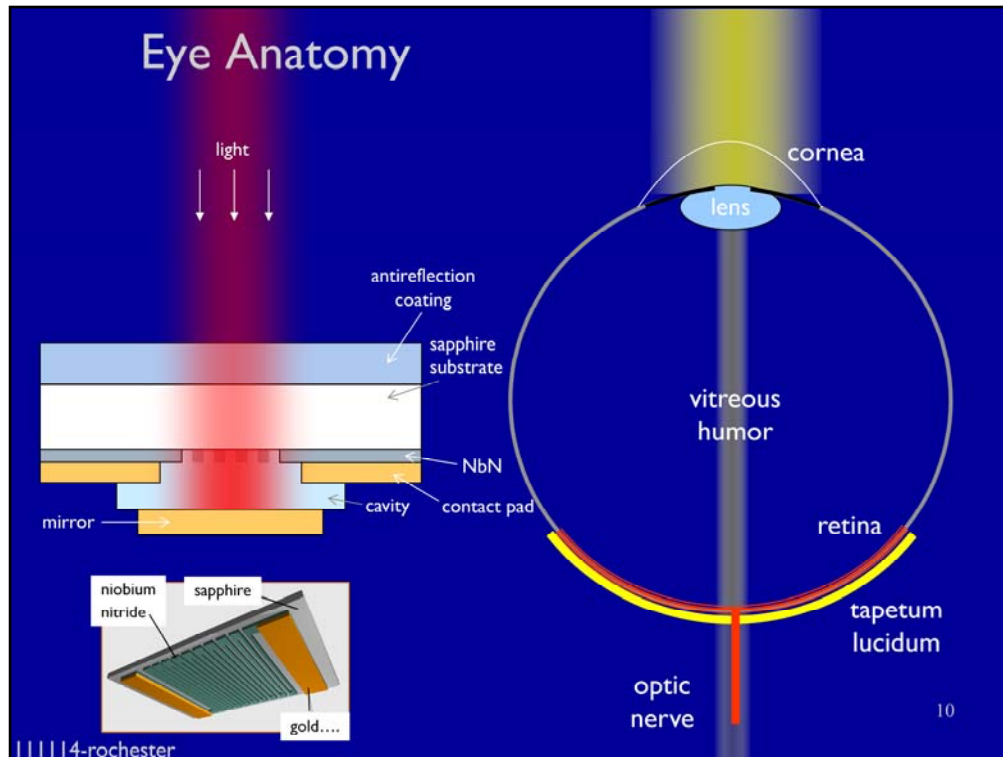
Bernstein and Pease, "Electron Microscopy of the Tapetum Lucidum of the Cat" *Journal of Cell Biology*, Vol. 5, 35-39, (1959)

9

Berggren

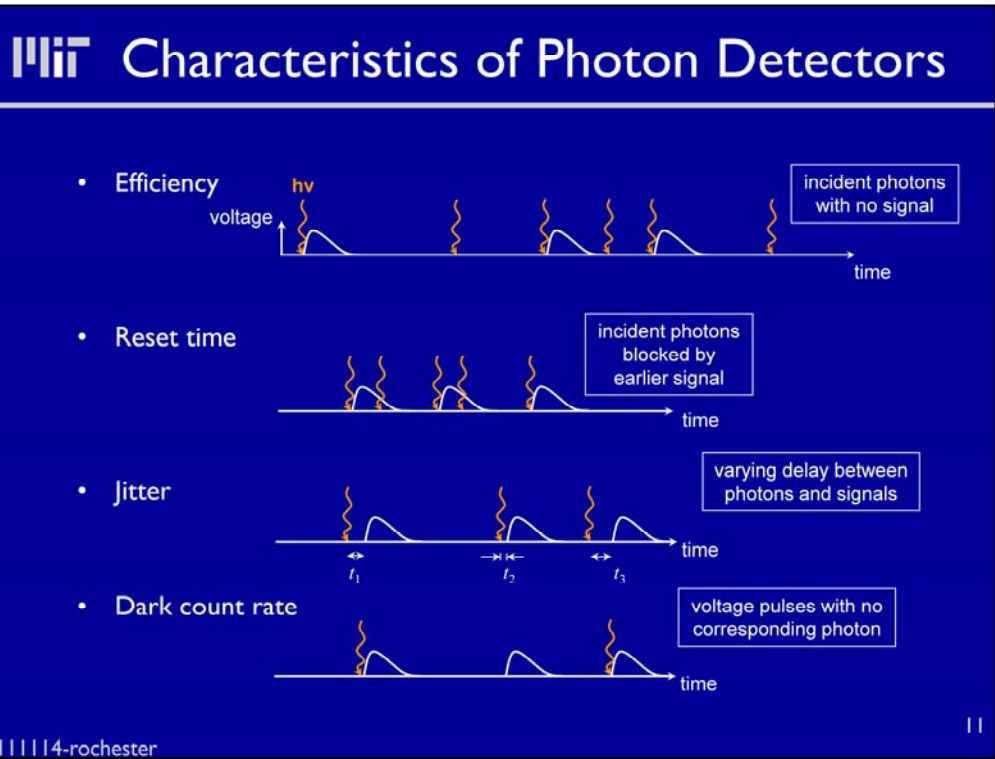
|||||4-rochester

It may also perhaps be surprising that evolution has equipped a cat's eye to recover some of the transmitted light through the retina with a layer of cells that reflects the transmitted light, giving it another opportunity for absorption.



Surprisingly, the human eye is a very good model for understanding the issues involved with low-level light detection.

The rods are the primary sensors for low light levels (the cones are responsible for color sensing). Rods can easily detect single photons, but to avoid shot noise, multiple rods must fire for the brain to interpret it as a signal. While ~ 300 photons illuminate the eye, reflection from the cornea, absorption in the eye, and transmission through the eye account for a huge total amount of loss ($> 90\%$). The result is that only a few photons are required to detect the fully dark-adapted eye.



SPD is a transducer that converts a very weak optical signal in an electronic signal.

This slide outlines the basics of photodetector metrics.

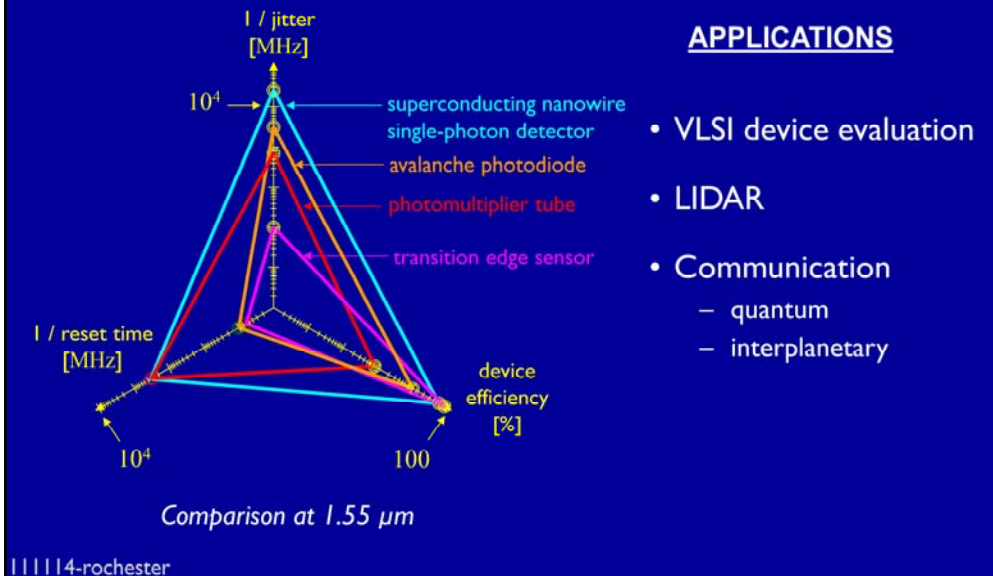
Efficiency tells us with what probability an incident photon results in a voltage pulse.

Reset time tells us how long we must wait after one voltage pulse before we can detect a second incident photon.

Jitter tells us the uncertainty in the arrival time of a voltage pulse after the arrival of a photon.

And dark counts tells us the probability that a voltage pulse will arise in the absence of a photon.

Nanowire Single-Photon Detector



Here is a technology comparison between various possible detectors, and an array of applications of interest.

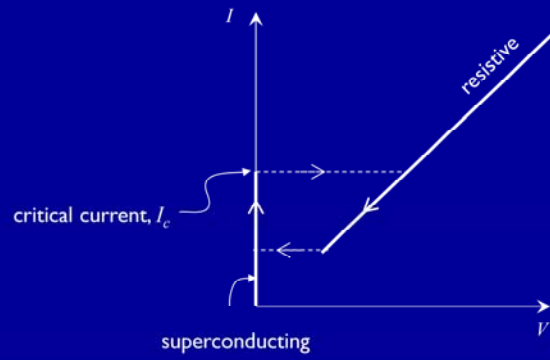
Slide 12

KB39 need references for VLSI and LADAR and quantum applications
Karl Berggren, 11/3/2008

DEVICE OPERATION

11114-rochester

Superconductive Nanowire Behavior

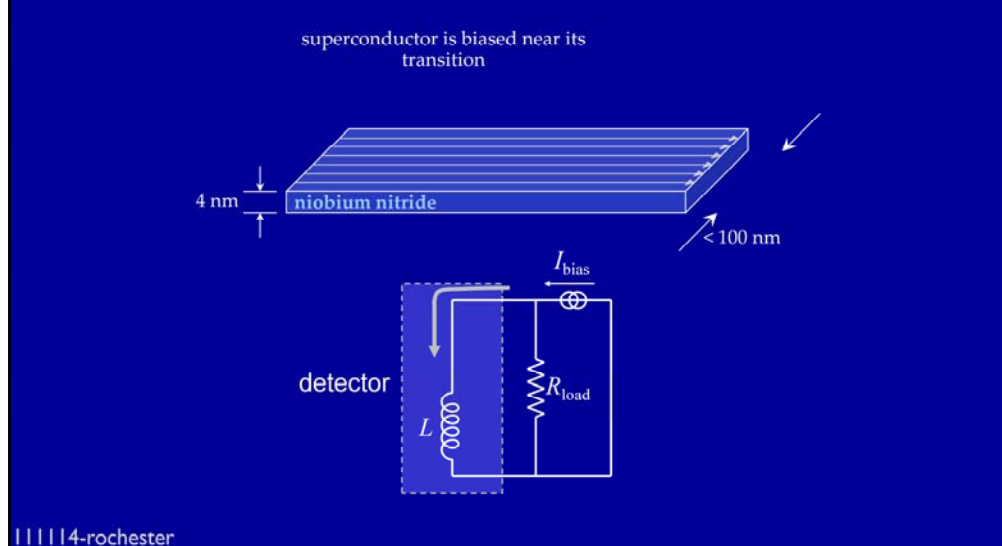


11114-rochester

Berggren

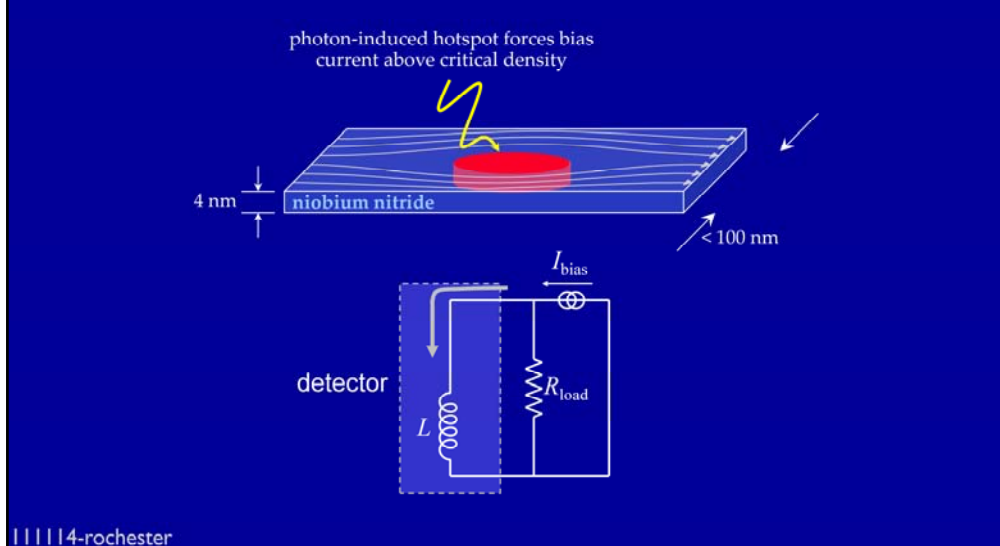
Basic current-voltage characteristic of a superconductor.

Detection Mechanism Explanation



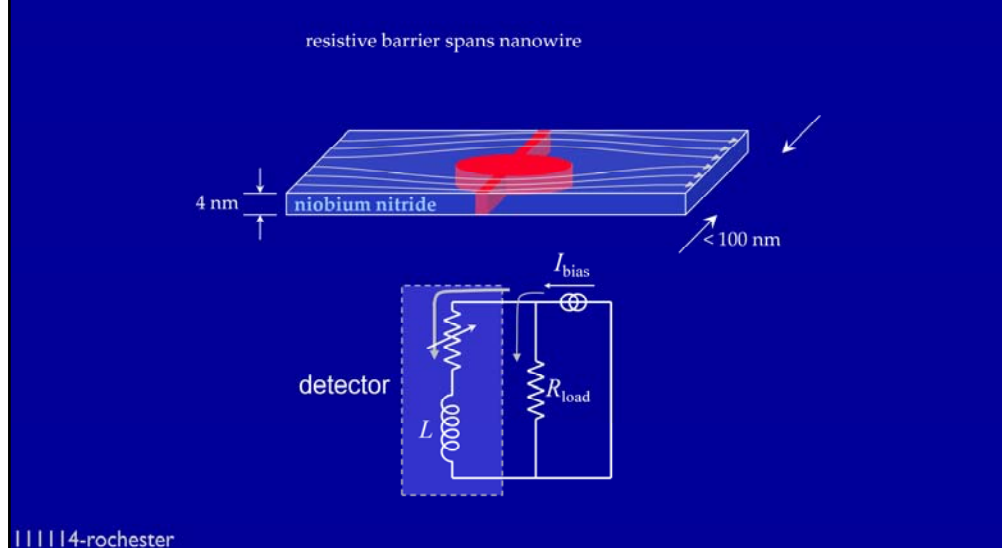
Schematic of sequence of operations of a superconducting wire, starting with current in nanowire.

Detection Mechanism Explanation



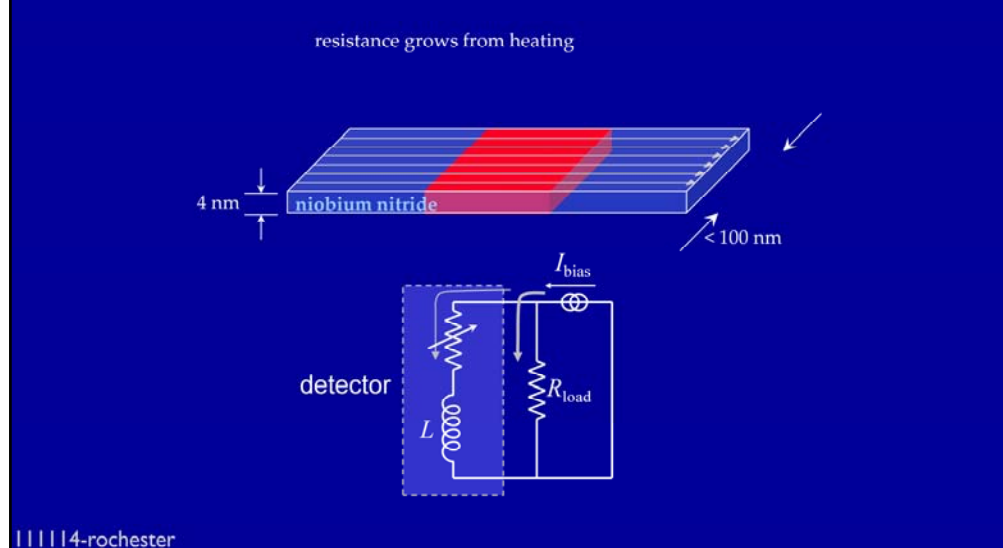
Photon hits, creating a hotspot (at least by some models). The current is diverted, increasing the current density around the wire.

Detection Mechanism Explanation



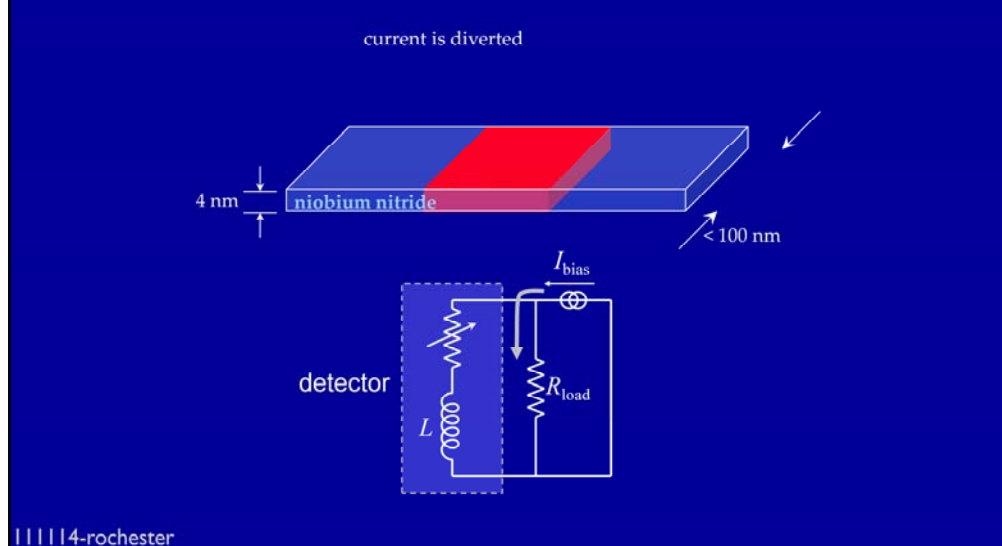
Critical current density is exceeded in the nanowire, current starts to be diverted to the load resistor

Detection Mechanism Explanation



Current in load resistor give signal, while current in detector results in heating

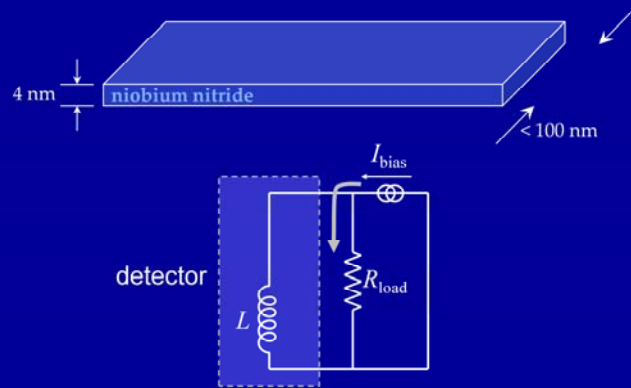
Detection Mechanism Explanation



Current is now gone from detector, and hot region starts to collapse

Detection Mechanism Explanation

superconductivity is restored



|||||4-rochester

Superconductivity is restored

kinetic inductance explained

karlberggren 1 videos [Subscribe](#)

i

$A \text{ e.m.f.} \rightarrow v$

$E_k = \frac{1}{2} M v^2$

$i = A n e v \Rightarrow v = \frac{i}{A n e}$

$E_k = \frac{1}{2}$

2:31 / 5:15

240p

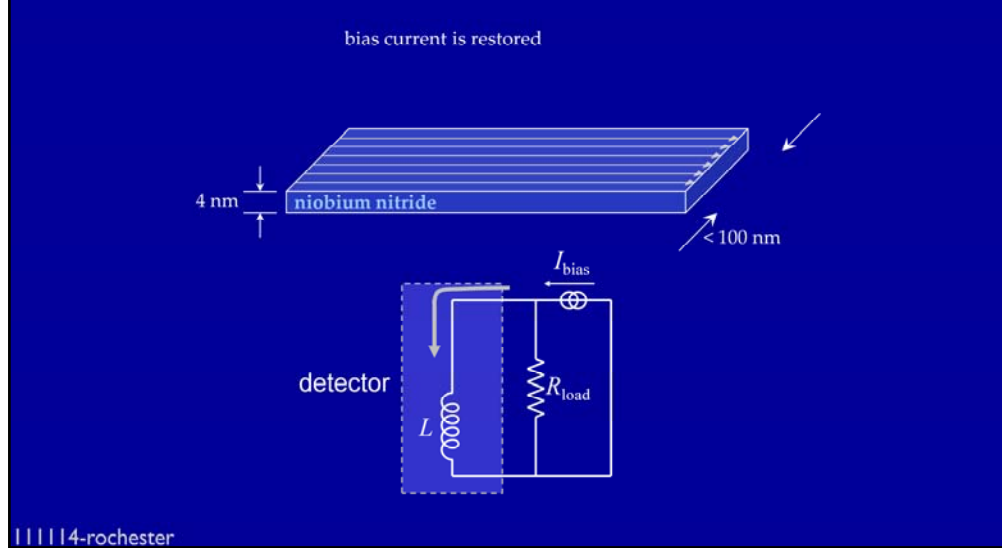
This video is public.

Suggestions

- For Ma... by tothe... 100,784
- Full Liv... Trailer by code... 16,161
- Observ... off-shel... by camo... 370 view
- Lec 23... and Ma... by MIT 29,603
- MIT Ph... Reson... by mitted... 119,443
- Lec 20

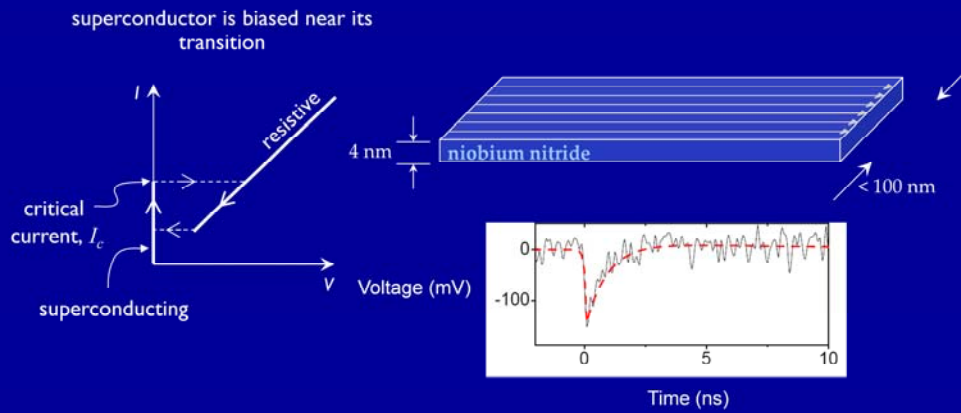
Kinetic inductance explained on youtube

Detection Mechanism Explanation



Supercurrent is eventually restored

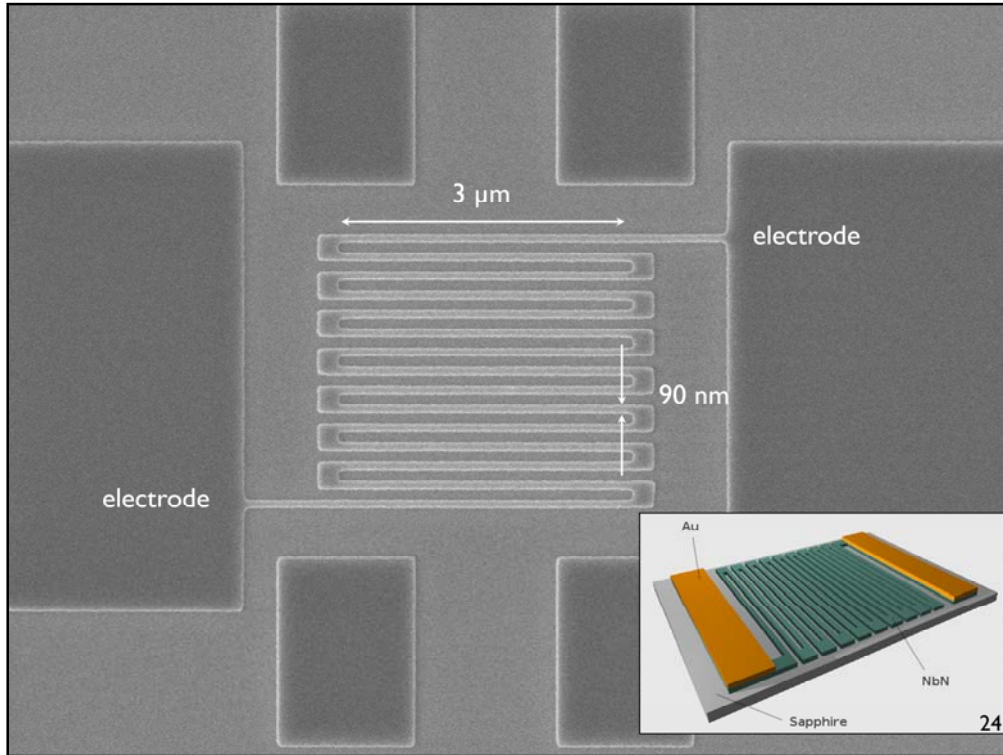
Detection Mechanism Explanation



Kerman, Dauler, Keicher, Yang, KB, Gol'tsman, Voronov, *Applied Physics Letters*, (2006)
111114-rochester

Same as previous slide, but the voltage pulse that corresponds to these events is shown in the bottom right. It is ~ 3 ns.

Of course, the wire is narrow, so a lot of light just misses it, which is optical loss.

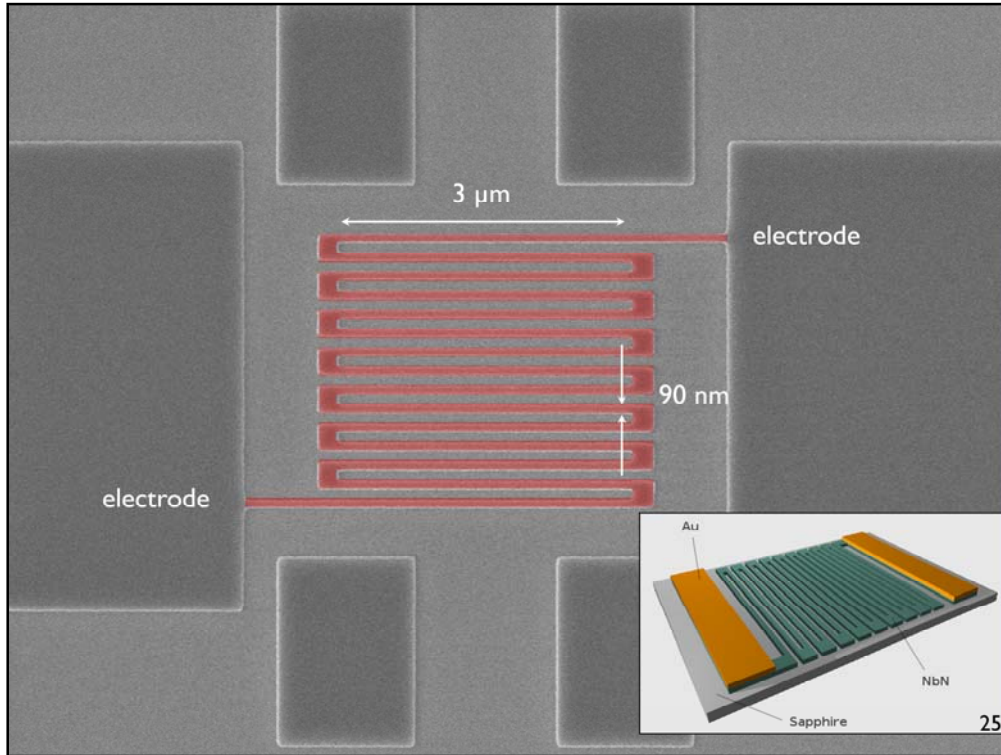


You might get optical loss with these devices from, for example, optical reflection and transmission, or with device constrictions. An important way around this loss is to maximize the area of overlap of the detector with the optical beam (without reducing the nanowire width). We accomplish this by winding the wire into a boustrophedonic (or “meander”) pattern as shown in this SEM. You still lose a fair amount of the light through the gaps between the wires, but a lot less than you would lose with just a single wire. You also gain a lot by reducing those gaps, which is something we’re working on. The loss through the gaps isn’t quite proportional as you might expect, because the structures are subwavelength.

A lot of light is still lost due to reflection and transmission, however, so we added some optical enhancements to the device.

KEYWORDS: SNSPD, photodetector, micrograph, SEM

TITLE: SEM of “standard” SNSPD

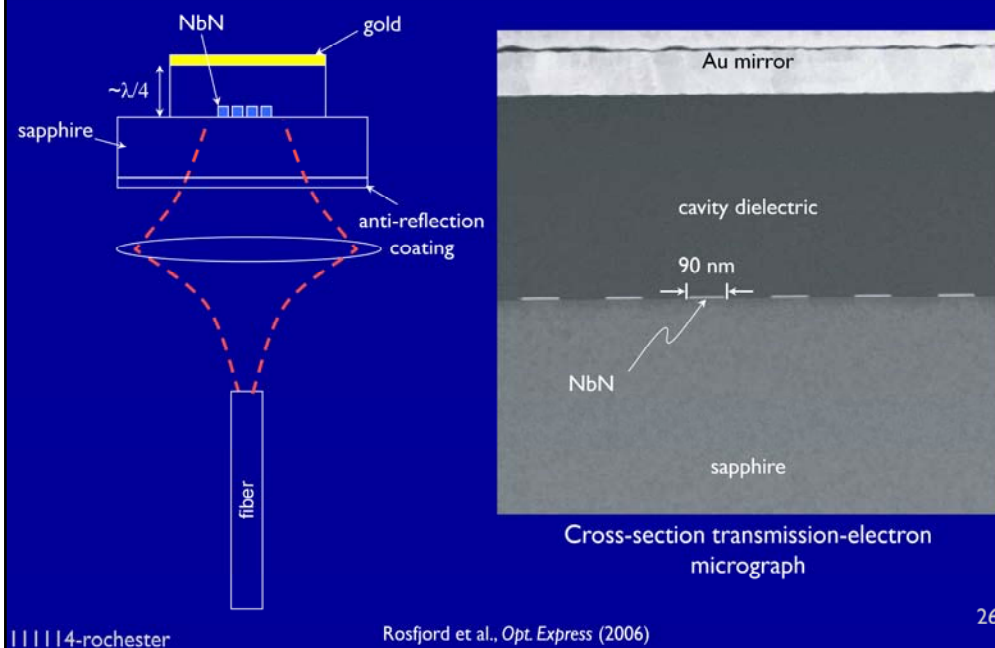


You might get optical loss with these devices from, for example, optical reflection and transmission, or with device constrictions. An important way around this loss is to maximize the area of overlap of the detector with the optical beam (without reducing the nanowire width). We accomplish this by winding the wire into a boustrophedonic (or “meander”) pattern as shown in this SEM. You still lose a fair amount of the light through the gaps between the wires, but a lot less than you would lose with just a single wire. You also gain a lot by reducing those gaps, which is something we’re working on. The loss through the gaps isn’t quite proportional as you might expect, because the structures are subwavelength.

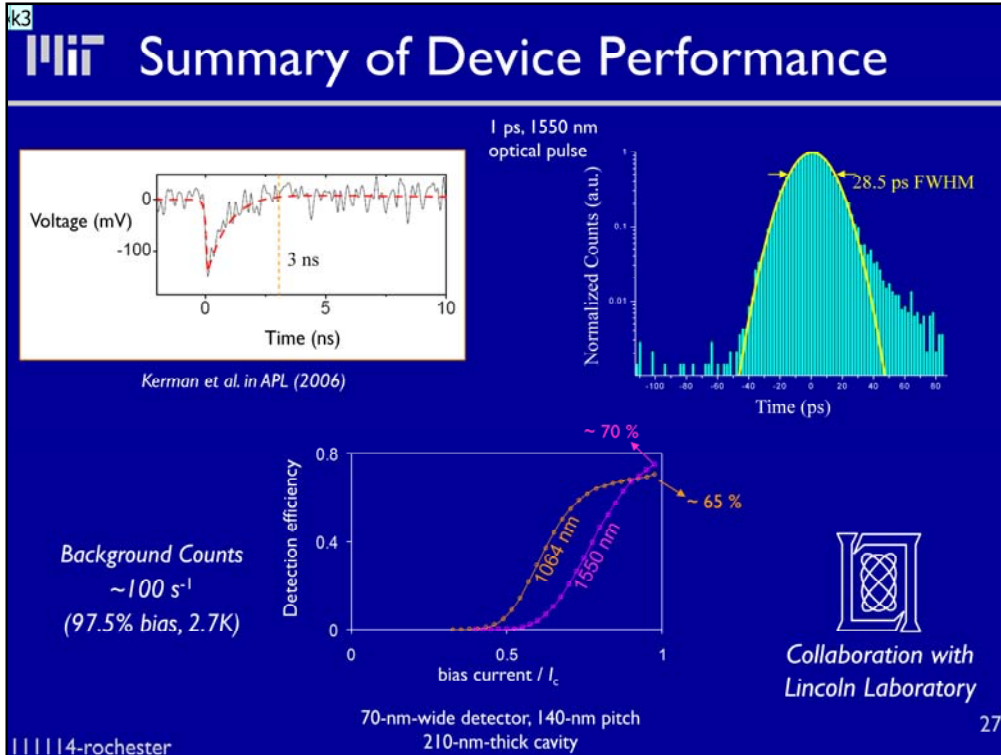
A lot of light is still lost due to reflection and transmission, however, so we added some optical enhancements to the device.

Miki NICT

SNSPD integrated in an optical cavity



Summary of the work published in Rosfjord Et. Al 2006, showing cavity resonator attached to detector.



Here we summarize the resulting detector performance, including a reset time of 3 ns, Stress that no gating is required and room temp el is sufficient a gaussian jitter of 30 ps, a detection efficiency of 57% 1.55 μm optical wavelength.

We have now also measured the dark counts. A 95% bias, we see 200 Hz, at 97.5% we see 600 Hz). These are spectacular numbers, but perhaps not as best as the very best reported to date. These numbers are limited by background light, not by true intrinsic dark counts, we believe.

No other competing technology offers all these 4 features at the same time.

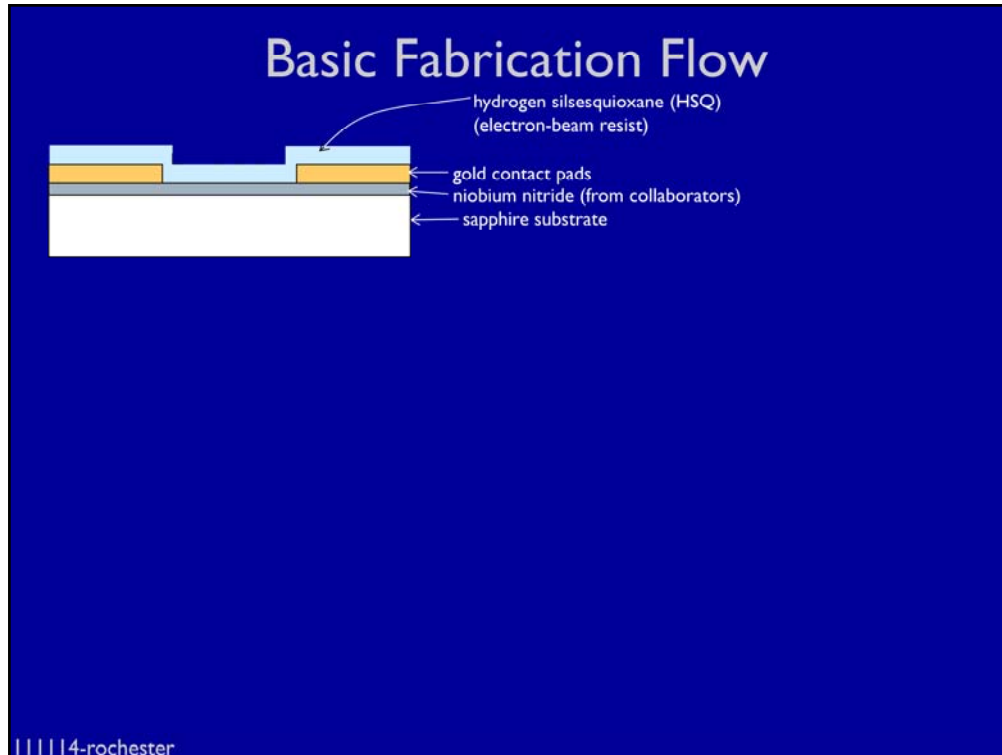
Slide 27

k2 update with nes data
karl, 4/19/2011

k3 de/DCR important for Qcomm
karl, 7/17/2011

FABRICATION

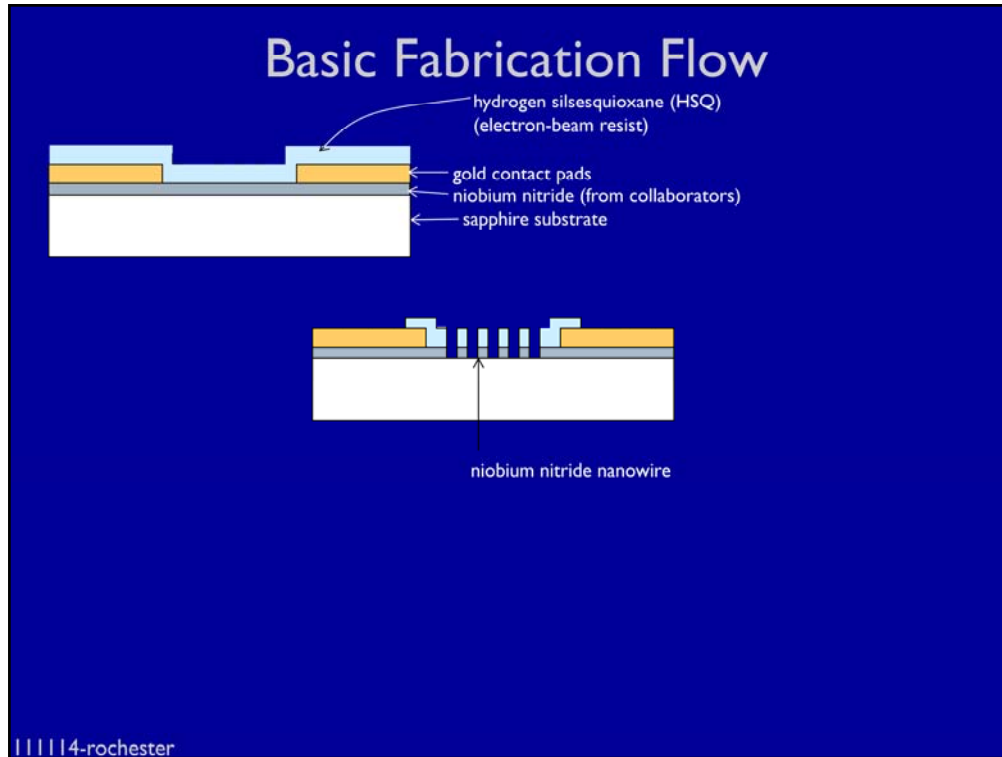
||||4-rochester



Here we have a sequence of images that show one after the other the fabrication process for the addition of the cavity. We start (upper left) with HSQ on the device, left over from patterning the nanowires; we then add (lower left) a cavity. It is self-planarized by the spin-on process. We next (upper right) add a gold mirror; finally (lower left) we add the underlying HSQ anti-reflection coating.

TITLE: Cavity fabrication process

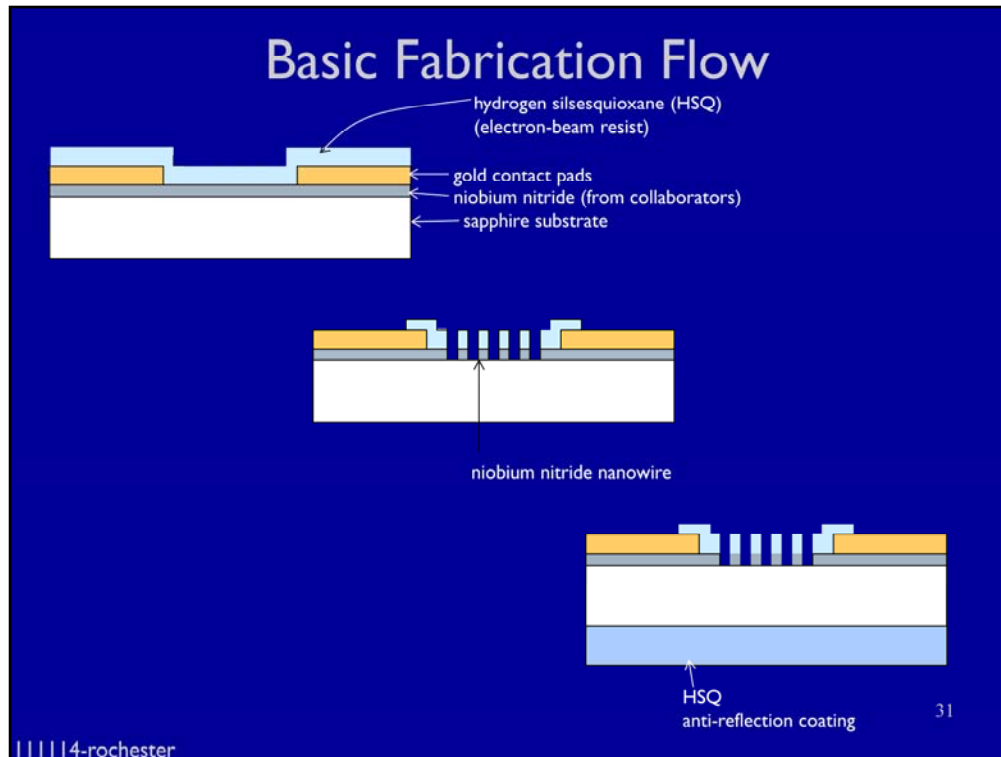
KEYWORDS: SNSPD, photodetector, schematic



Here we have a sequence of images that show one after the other the fabrication process for the addition of the cavity. We start (upper left) with HSQ on the device, left over from patterning the nanowires; we then add (lower left) a cavity. It is self-planarized by the spin-on process. We next (upper right) add a gold mirror; finally (lower left) we add the underlying HSQ anti-reflection coating.

TITLE: Cavity fabrication process

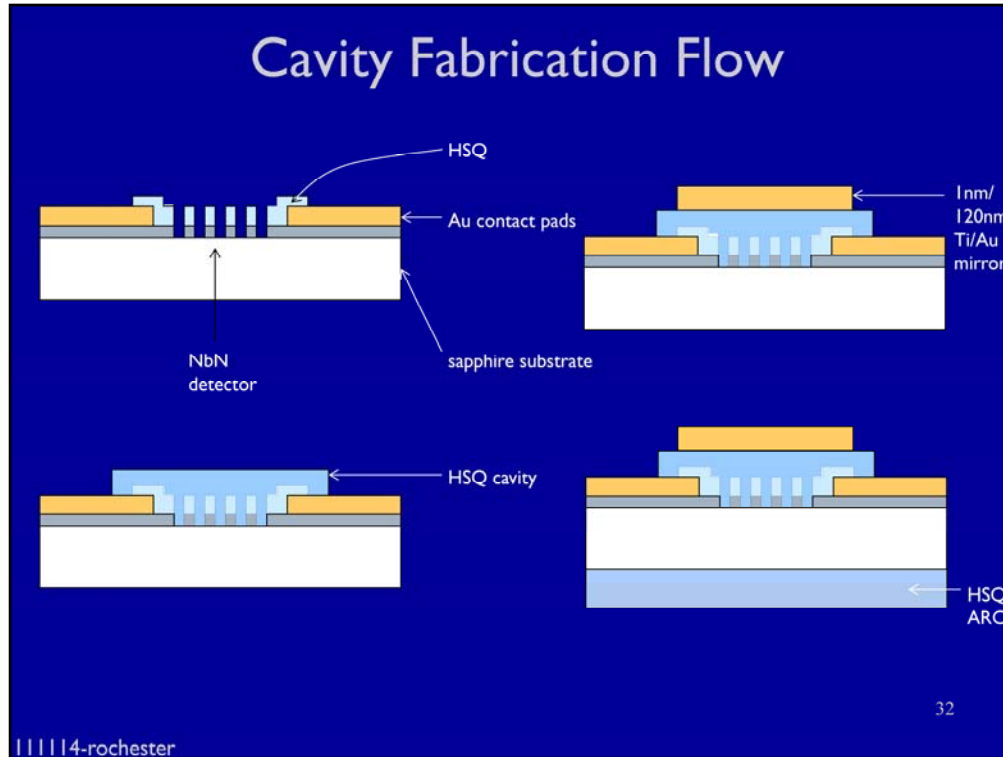
KEYWORDS: SNSPD, photodetector, schematic



Here we have a sequence of images that show one after the other the fabrication process for the addition of the cavity. We start (upper left) with HSQ on the device, left over from patterning the nanowires; we then add (lower left) a cavity. It is self-planarized by the spin-on process. We next (upper right) add a gold mirror; finally (lower left) we add the underlying HSQ anti-reflection coating.

TITLE: Cavity fabrication process

KEYWORDS: SNSPD, photodetector, schematic



Here we have a sequence of images that show one after the other the fabrication process for the addition of the cavity. We start (upper left) with HSQ on the device, left over from patterning the nanowires; we then add (lower left) a cavity. It is self-planarized by the spin-on process. We next (upper right) add a gold mirror; finally (lower left) we add the underlying HSQ anti-reflection coating.

TITLE: Cavity fabrication process

KEYWORDS: SNSPD, photodetector, schematic

APPLICATION

Transition slide

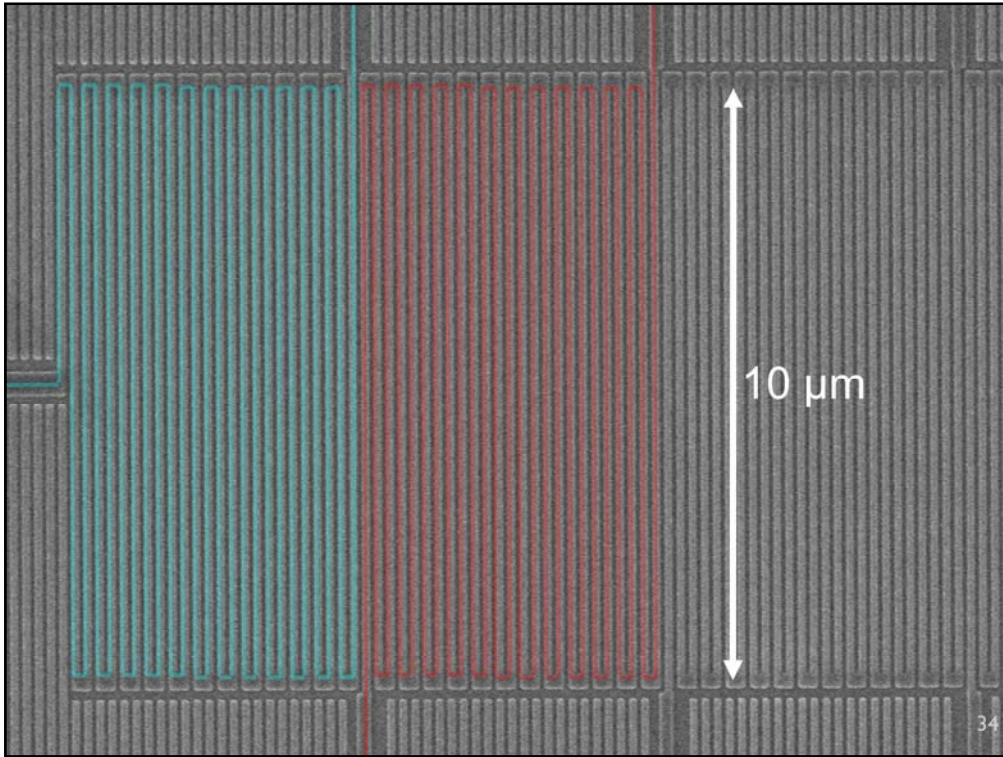
That was the performance of the detectors now

What do we do with these detectors?

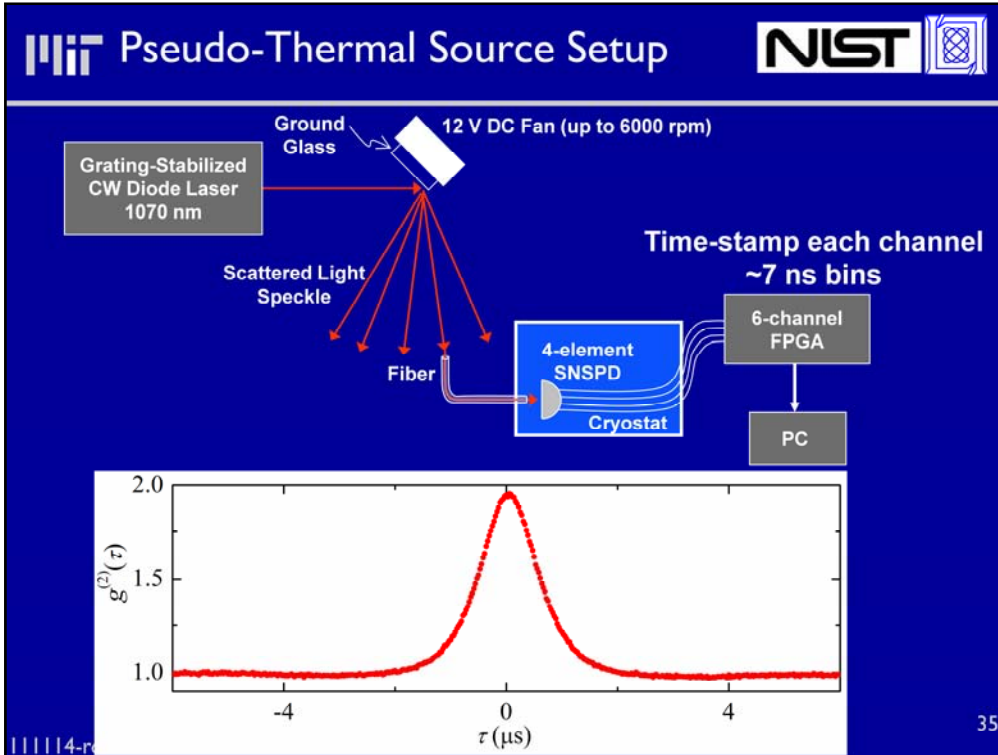
In the following slides you will see an application. The following experiments were carried out by Dauler from LL Stevens Mirin from NIST with devices from Berggren lab

Slide 33

FM8 mention Dauler Stevens and Mirin
Francesco Marsili, 4/26/2011



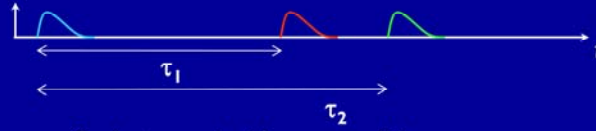
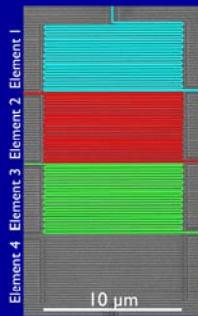
This is just a close-up SEM of a linear quad array, illustrating the geometric configuration, as well as the quality of the fabrication.



We can simulate a thermal source by shining a coherent source onto a rotating piece of ground glass. The scatter destroys the spatial coherence of the source, resulting in a pseudo-thermal source. The result is then passed into the 4-element SNSPD, and correlations are examined.



3-photon coincidences



2-photon coincidence conditions:

$$\tau_1 = 0$$

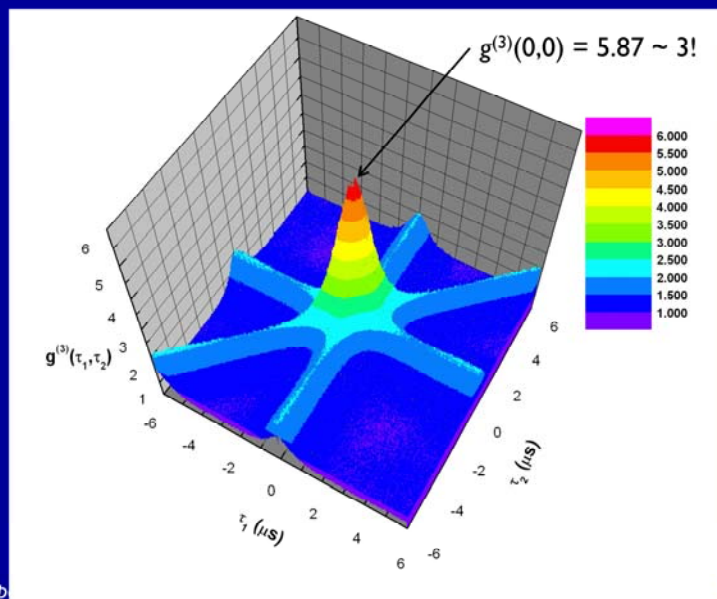
$$\tau_2 = 0$$

$$\tau_1 = \tau_2$$

3-photon coincidence :

$$\tau_1 = \tau_2 = 0$$

They went further and measured higher order correlation functions.



"High-order temporal correlations in a quantum state"
Berggren, Mirin, and Nam, *Optics Express*, 18, 1430 (2010)
111114-rochester

Hamilton,

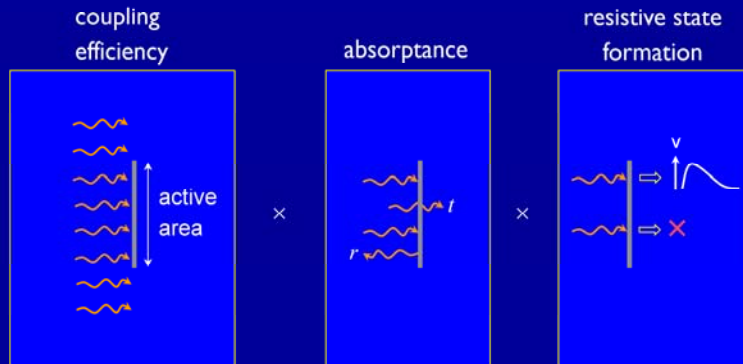
The light was bunched so the 2 and 3 ph coincidences have higher probability. As you see the g_3 has local maxima where the conditions for a 2ph coincidence is satisfied and a absolute maximum for a 3 ph coincidence.

NANO-ANTENNAE

|||||4-rochester

Transition slide

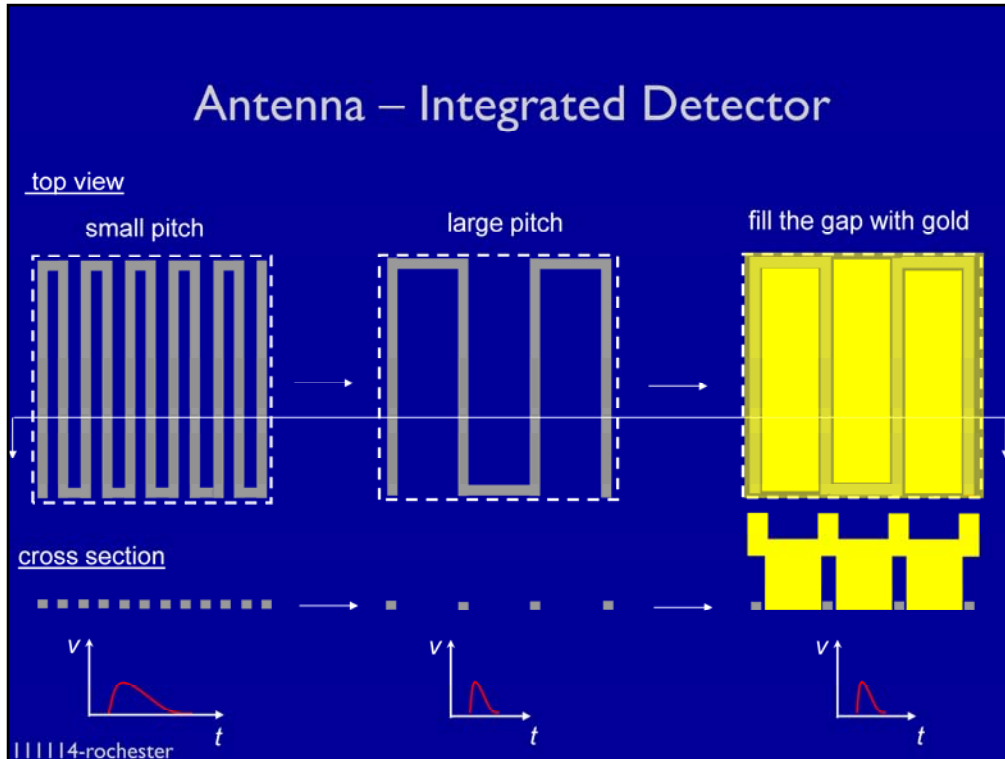
The Three Keys to Efficiency



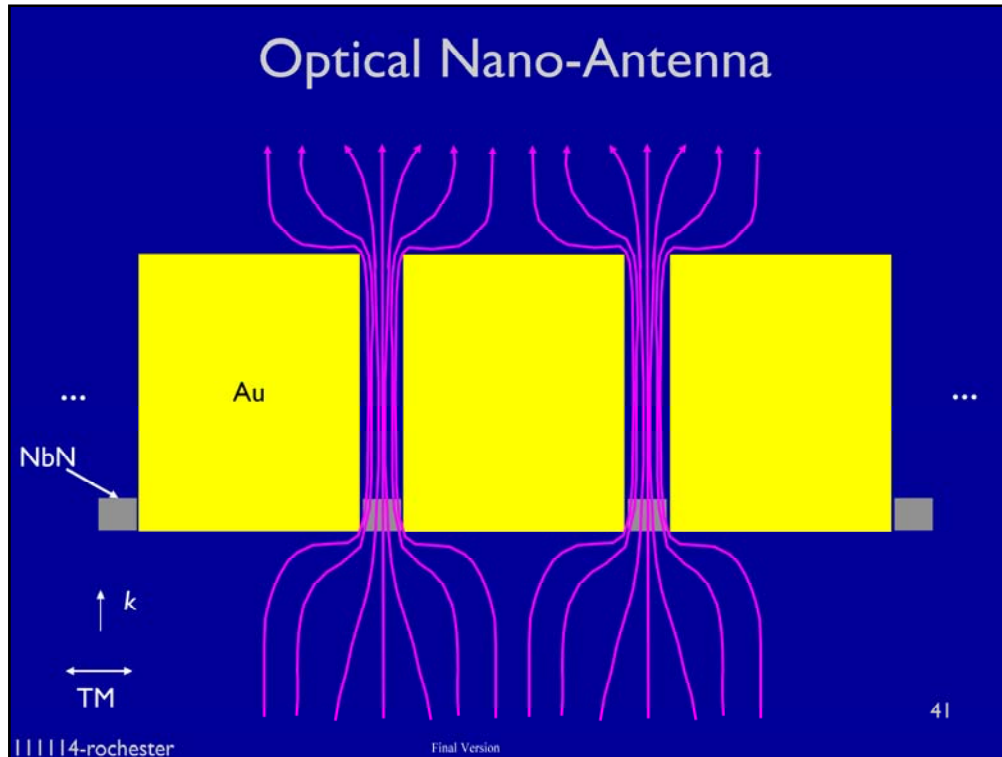
39

|||||4-rochester

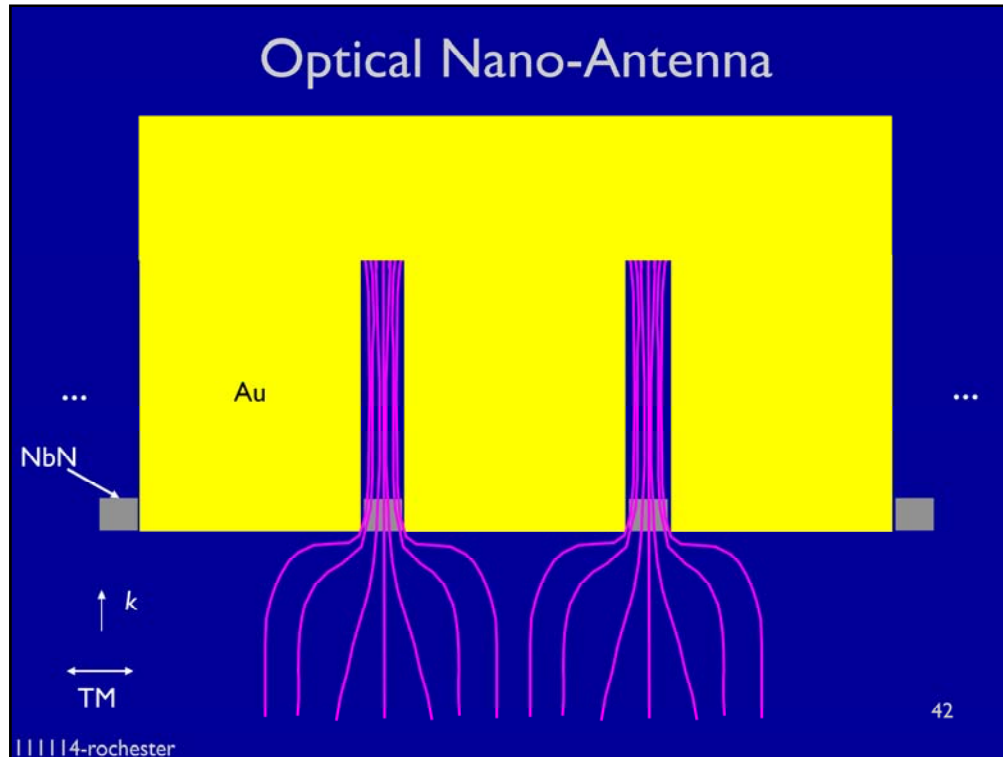
These are the keys to detector efficiency. You need a large active area, a high absorbance, and a high probability that an absorbed photon will lead to the formation of a resistive state. The importance of these contributors is summarized in the formula below. We observe that a graph of normalized DE vs. absorbance will give a slope of the probability of resistive-state formation.



Our idea is simple. Here is NbN meander, we fill the gaps between NbN with gold, and expand the area by only expanding the gold part. In this way, we can increase the effective area of the detector without increasing the length of the nanowire. It is natural to ask the following question? In this structure, can NbN effectively absorb the incident photons?

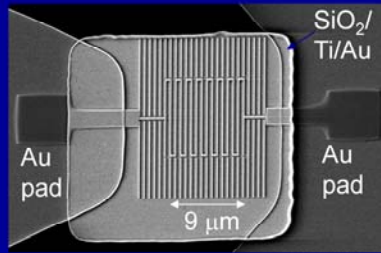


One of the basic operating principles of this devices is that the field intensifies as it goes through a narrowing slit. This design is analogous to a “feed gap” in conventional antennae, but here the principle is used at the nanoscale.



The light is squeezed into the gaps between gold so that the overlap between the light and NbN is large. Thus we expect strong absorption.

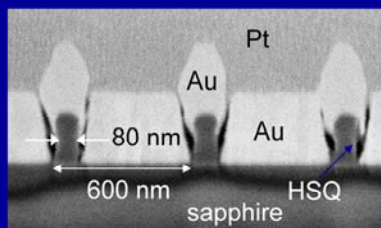
Fabrication



fabrication challenges

- e-beam writing on thick HSQ
- gold migration in evaporation

ion-beam cross-section

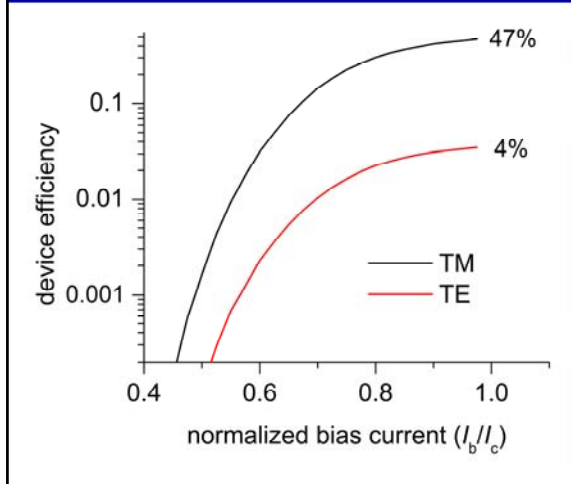


111114-rochester

We fabricated the device. This is the cross section. The pitch is 600 nm and the width of the nanowire is 80 nm. The fabrication challenges include e-beam writing directly on thick HSQ and e-beam evaporation, in which the gold might migrate, creating defects like this.

Nano-Optical Antenna for Nanowire Detectors

- Nano-antennae improve collection, permitting 3 x area, with same reset time



- 600-nm pitch, 9- μm -by-9- μm area
- 47% device efficiency
- 5 ns reset time

Hu et. Al. *Optics Express*, 2010

111114-rochester

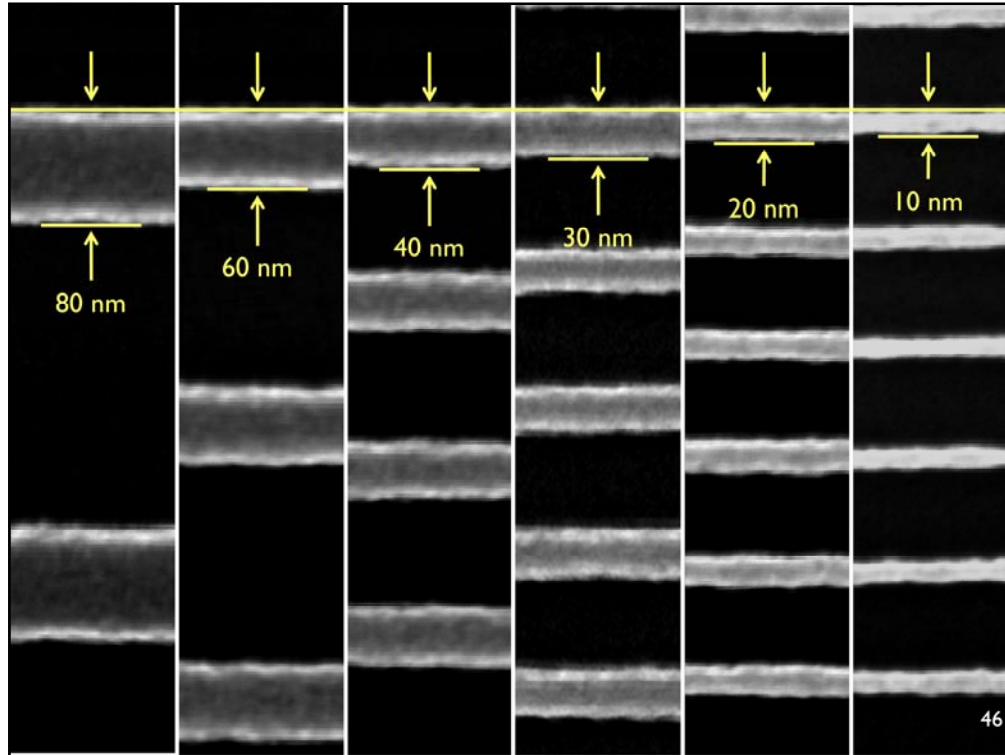
We performed EM simulation. The yellow arrows represent the poynting vector. The gold can effectively collect the light and focus onto the NbN nanowire. The brightness represents the intensity of the fields, which is strongest at the location of NbN. Here I show the cross section image of the device, and the width of the nanowire is 80 nm and the pitch is 600 nm. With this stucture, we get a 3 x larger area with the same length of nanowire and same reset time, and the efficiency is 47%.

SUB-30-NM DEVICES

|||||4-rochester

45

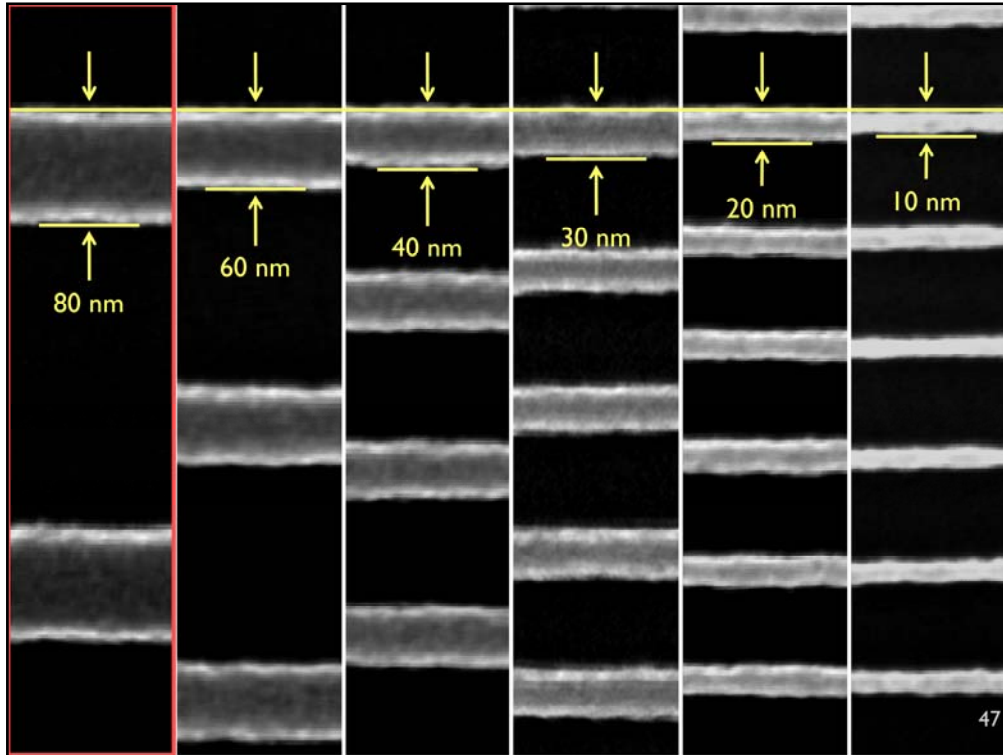
Transition slide



We developed a process that allows us to fab nw of width ranging from 80 to 10 nm with homogeneous x section over μms .

For us narrow means 30 nm and below.

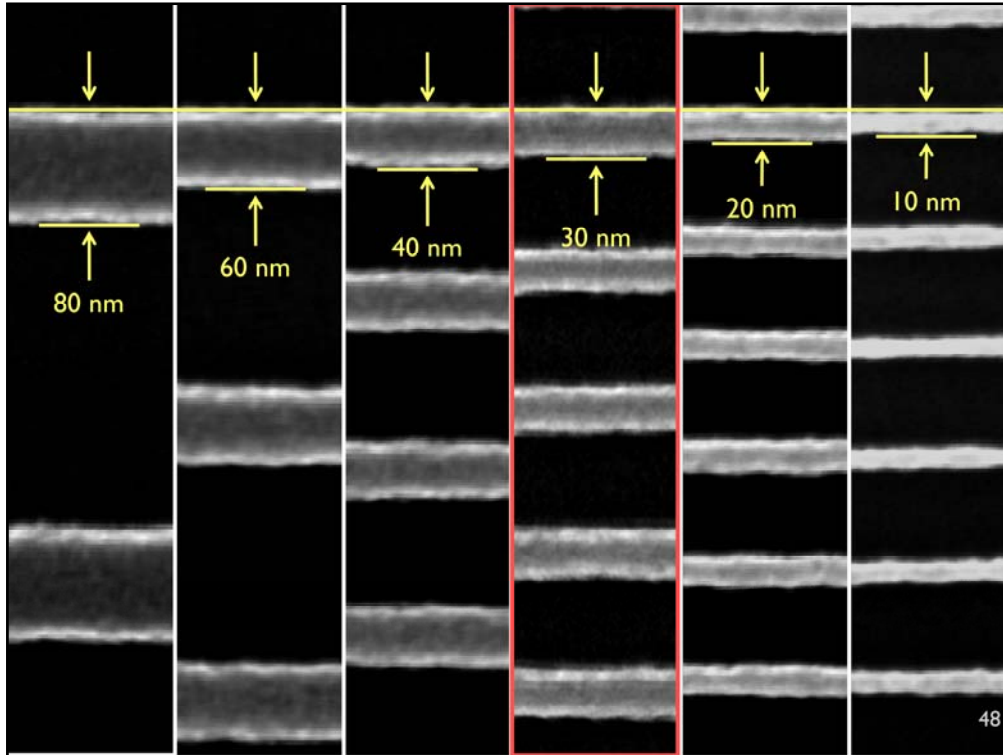
Scanning electron microscope (SEM) images of hydrogen silsesquioxane (HSQ) nanowires on a 4 nm-thick NbN film. The nanowires have different widths ($w= 10, 20, 30, 40, 50, 60, 80$ nm) and are arranged in a meander pattern with the same fill factor ranging from 30% to 12.5%. These structures were obtained by electron beam lithography (30 kV acceleration voltage) on 45 nm-thick HSQ.



We developed a process that allows us to fab nw of width ranging from 80 to 10 nm with homogeneous x section over ums.

For us narrow means 30 nm and below.

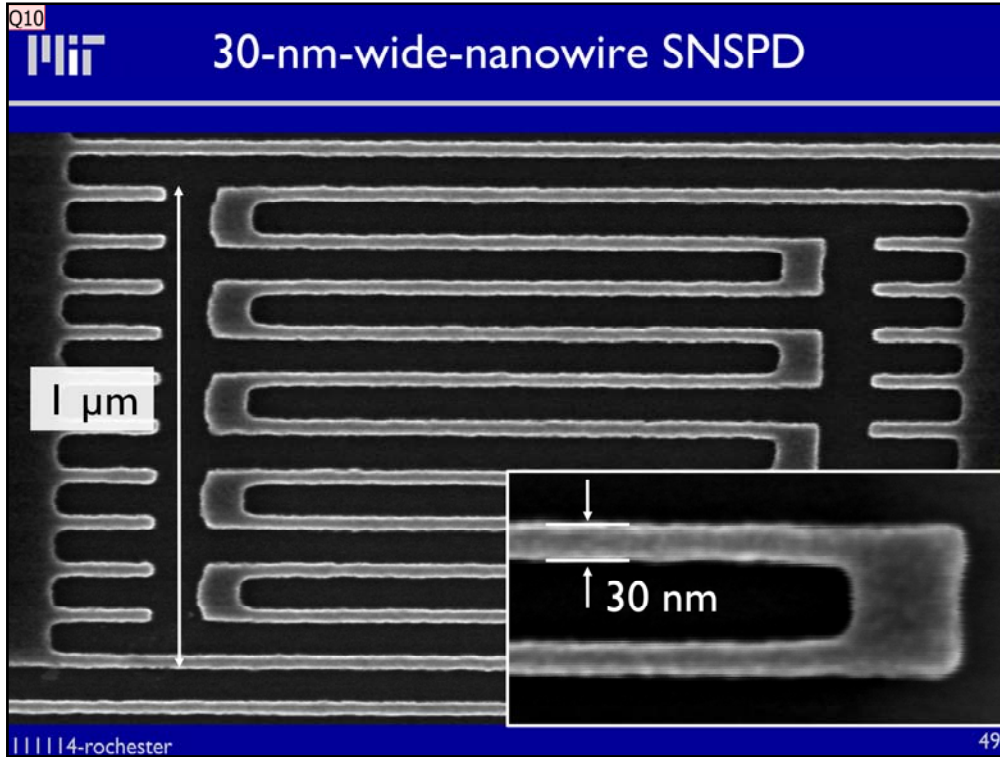
Scanning electron microscope (SEM) images of hydrogen silsesquioxane (HSQ) nanowires on a 4 nm-thick NbN film. The nanowires have different widths ($w= 10, 20, 30, 40, 50, 60, 80$ nm) and are arranged in a meander pattern with the same fill factor ranging from 30% to 12.5%. These structures were obtained by electron beam lithography (30 kV acceleration voltage) on 45 nm-thick HSQ.



We developed a process that allows us to fab nw of width ranging from 80 to 10 nm with homogeneous x section over μms .

For us narrow means 30 nm and below.

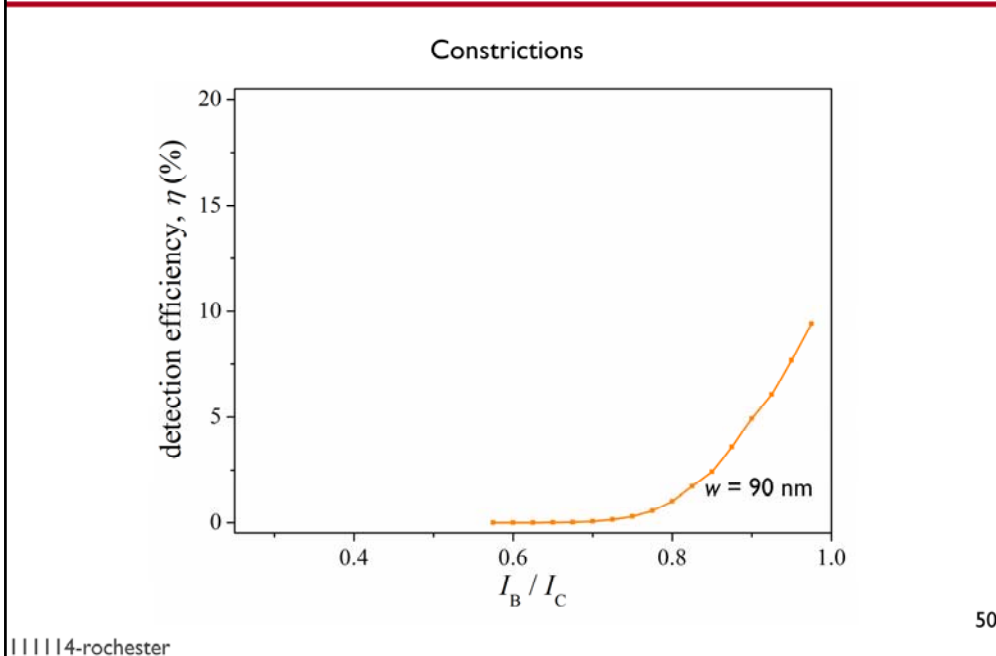
Scanning electron microscope (SEM) images of hydrogen silsesquioxane (HSQ) nanowires on a 4 nm-thick NbN film. The nanowires have different widths ($w= 10, 20, 30, 40, 50, 60, 80$ nm) and are arranged in a meander pattern with the same fill factor ranging from 30% to 12.5%. These structures were obtained by electron beam lithography (30 kV acceleration voltage) on 45 nm-thick HSQ.



Now let's see how a 30nm wide snsps behaves.
Scanning electron microscope (SEM) images of hydrogen silsesquioxane (HSQ) nanowires on a 4-nm-thick NbN film. The nanowires are 30-nm wide and are arranged in a meander pattern with 100-nm pitch. This structures was obtained by electron beam lithography (30 kV acceleration voltage) on 45-nm-thick HSQ.

Slide 49

Q10 4x4um2 device
QNN, 4/22/2011

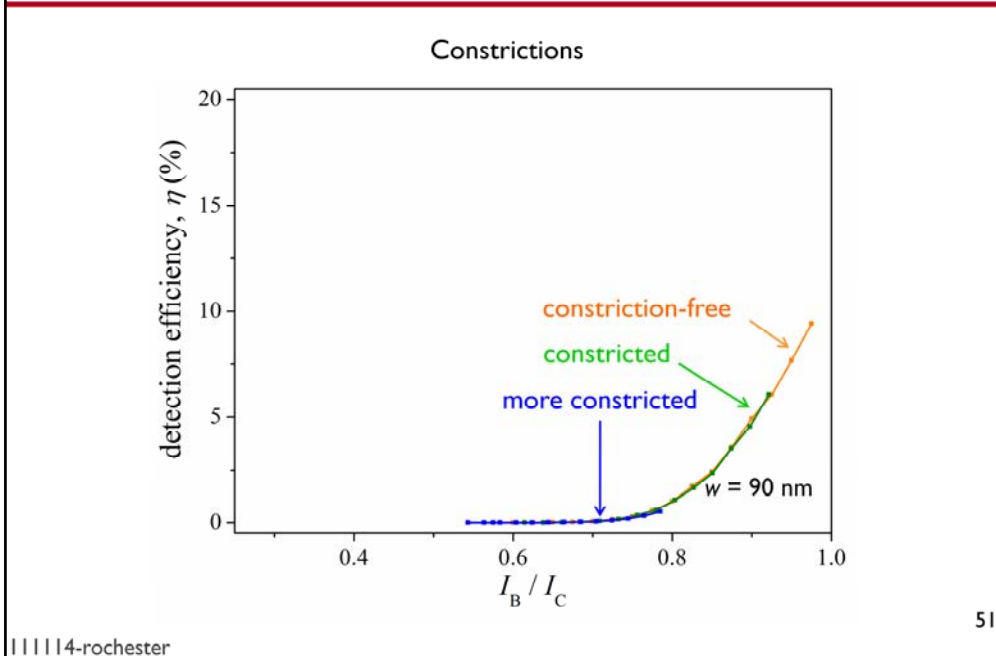


Lets 1st consider a 90 nm nanowire width SNSPD. The DE increases exponentially with the bias current. But the nanowire may have a constriction along its length. A defect where the superconductivity is suppressed and the IC is lower. This constriction limits the IC of the whole device so a constricted device cannot be biased up to the IC. So we lose DE exponentially.

Slide 50

- Q11** green change
QNN, 4/22/2011
- Q28** if flat part is abs liimit 100% DE achievable
QNN, 4/26/2011
- Q30** give physical picture of lower Ico
QNN, 4/26/2011

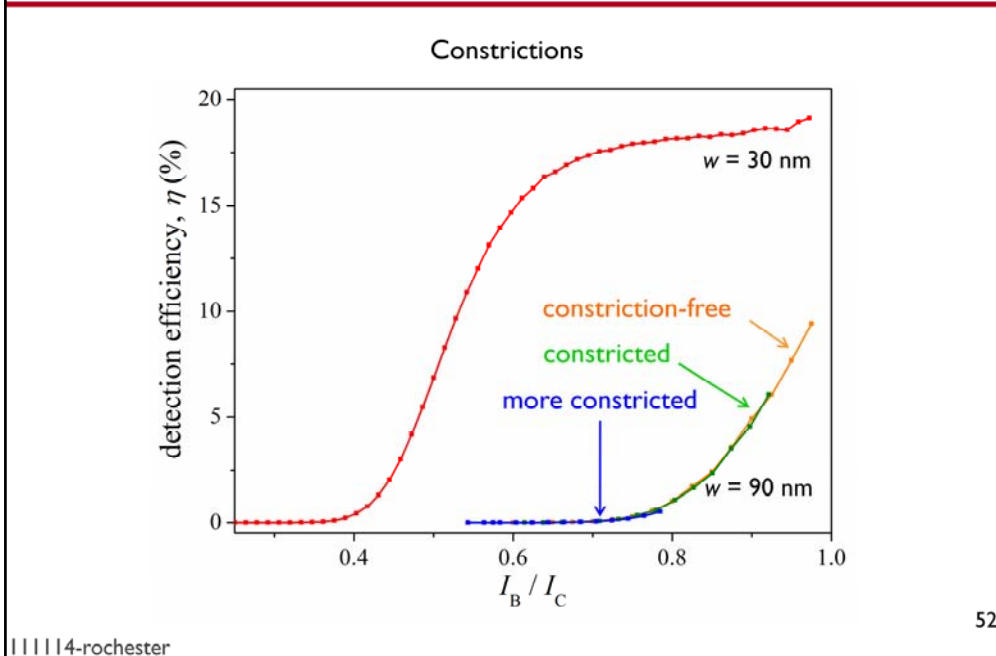
Standard vs Ultranarrow-Nanowire SNSPDs



Lets 1st consider a 90 nm nanowire width SNSPD. The DE increases exponentially with the bias current. But the nanowire may have a constriction along its length. A defect where the superconductivity is suppressed and the IC is lower. This constriction limits the IC of the whole device so a constricted device cannot be biased up to the IC. So we lose DE exponentially.

Slide 51

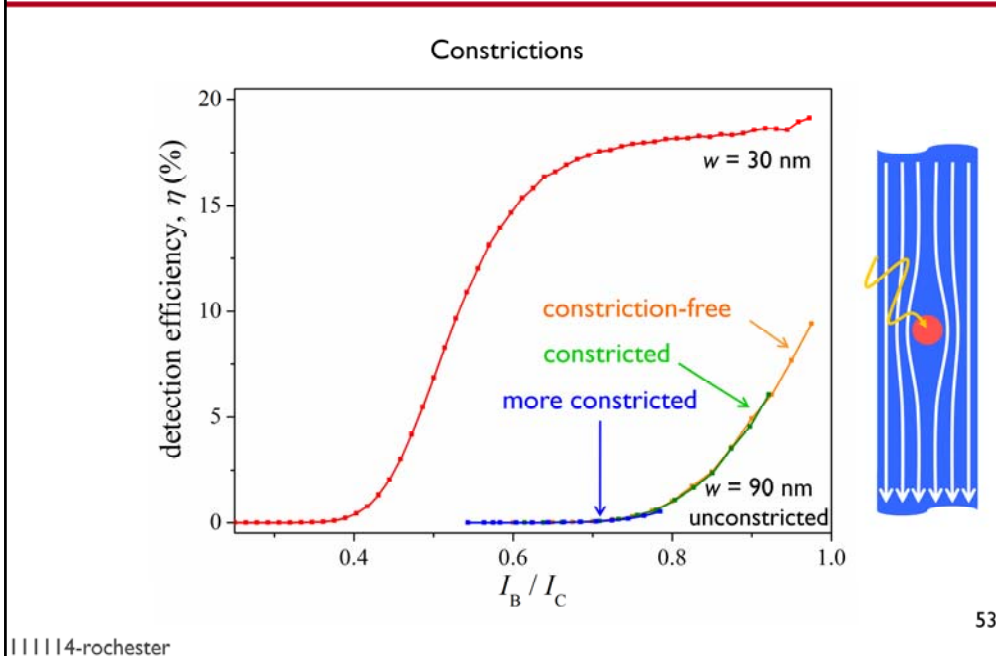
- Q41** green change
QNN, 4/22/2011
- Q42** if flat part is abs liimit 100% DE achievable
QNN, 4/26/2011
- Q43** give physical picture of lower Ico
QNN, 4/26/2011
- k4** simplify use of sigma
karl, 7/18/2011



Lets 1st consider a 90 nm nanowire width SNSPD. The DE increases exponentially with the bias current. But the nanowire may have a constriction along its length. A defect where the superconductivity is suppressed and the IC is lower. This constriction limits the IC of the whole device so a constricted device cannot be biased up to the IC. So we lose DE exponentially.

Slide 52

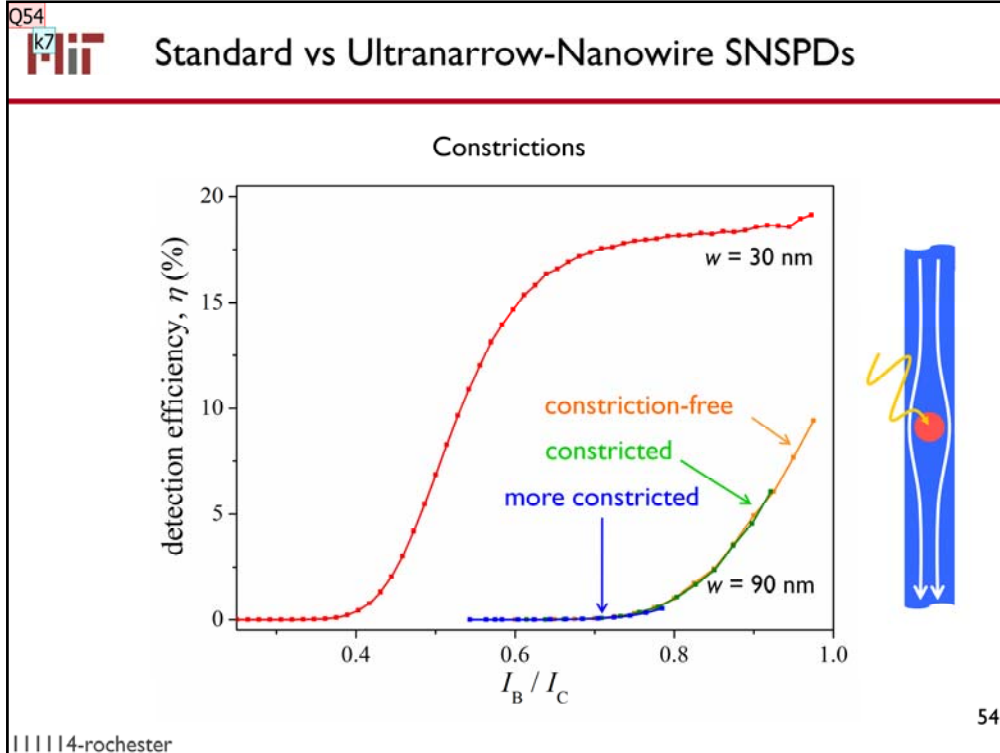
- Q47** green change
QNN, 4/22/2011
- Q48** if flat part is abs liimit 100% DE achievable
QNN, 4/26/2011
- Q49** give physical picture of lower Ico
QNN, 4/26/2011



Lets 1st consider a 90 nm nanowire width SNSPD. The DE increases exponentially with the bias current. But the nanowire may have a constriction along its length. A defect where the superconductivity is suppressed and the IC is lower. This constriction limits the IC of the whole device so a constricted device cannot be biased up to the IC. So we lose DE exponentially.

Slide 53

- Q56** green change
QNN, 4/22/2011
- Q57** if flat part is abs liimit 100% DE achievable
QNN, 4/26/2011
- Q58** give physical picture of lower Ico
QNN, 4/26/2011

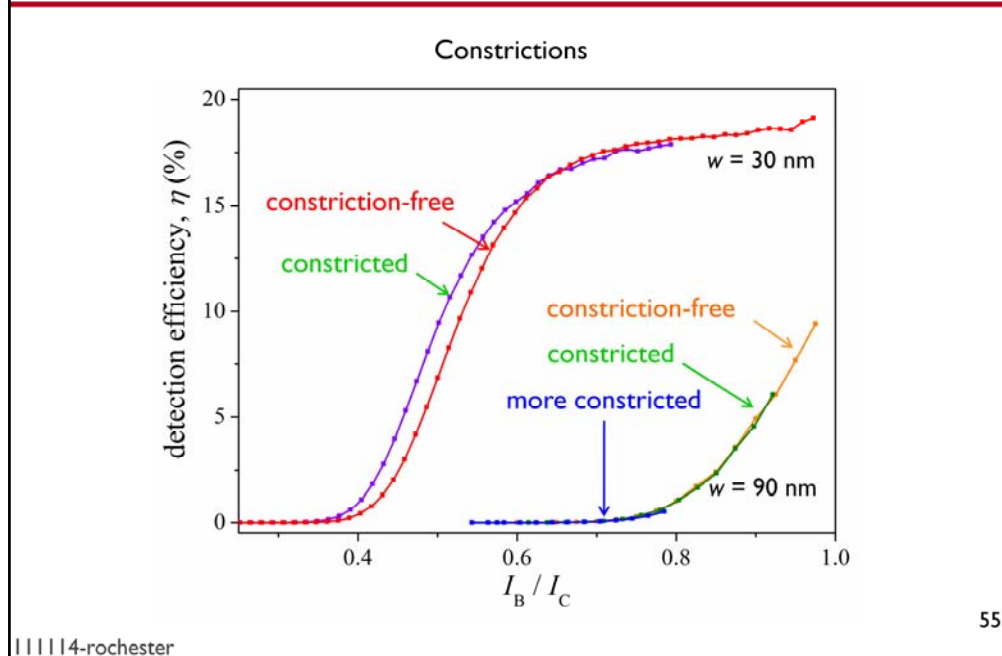


Lets 1st consider a 90 nm nanowire width SNSPD. The DE increases exponentially with the bias current. But the nanowire may have a constriction along its length. A defect where the superconductivity is suppressed and the IC is lower. This constriction limits the IC of the whole device so a constricted device cannot be biased up to the IC. So we lose DE exponentially.

The intuitive explanation of this effect is that the perturbation created by the abs of a ph does not depend on the nanowire width but only the ph energy so switching to a narrower nanowire the perturbation will affect a larger portion of the nanowire xsection.

Slide 54

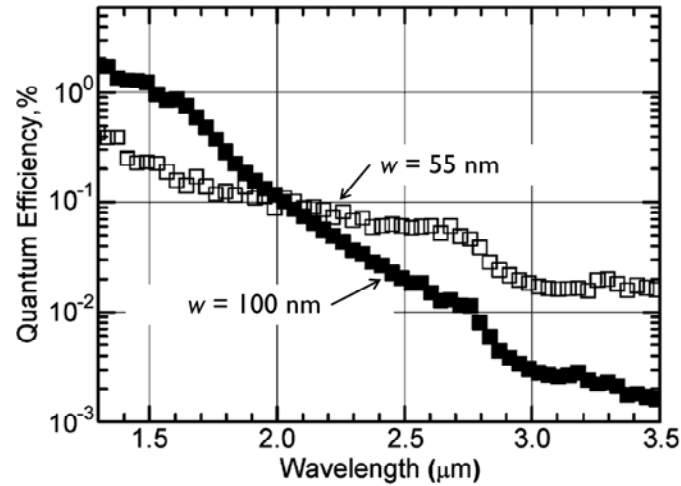
- Q53** **green change**
QNN, 4/22/2011
- Q54** **if flat part is abs liimit 100% DE achievable**
QNN, 4/26/2011
- k7** **mention bare device**
karl, 7/18/2011



Lets 1st consider a 90 nm nanowire width SNSPD. The DE increases exponentially with the bias current. But the nanowire may have a constriction along its length. A defect where the superconductivity is suppressed and the IC is lower. This constriction limits the IC of the whole device so a constricted device cannot be biased up to the IC. So we lose DE exponentially.

100% DE would be of use for linear optics quantum computing

Negligible responsivity above 2 μm

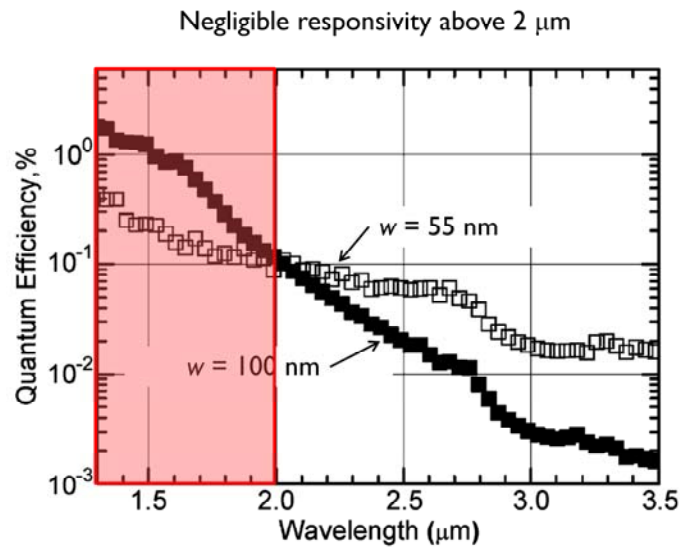


Example of results from Gol'tsman's paper on infrared detector sensitivity

Slide 56

Q59 goltsman paper
QNN, 4/26/2011

Standard vs Ultranarrow-Nanowire SNSPDs



Example of results from Gol'tsman's paper on infrared detector sensitivity

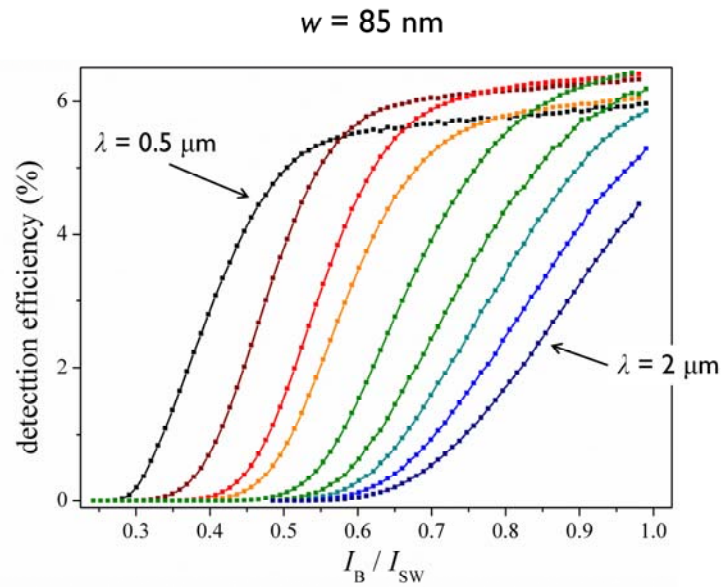
Slide 57

Q61 goltsman paper
 QNN, 4/26/2011

Q62 gray out range
 QNN, 4/29/2011



Detection efficiency vs I_B and wavelength

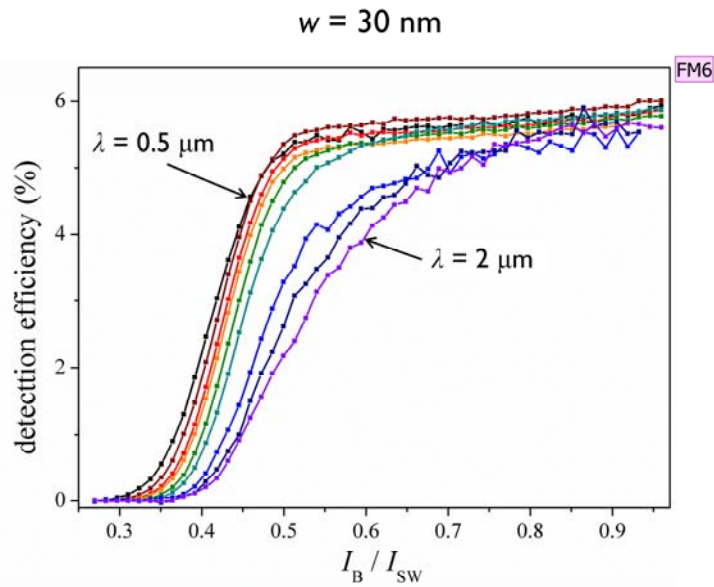


58

Here we have comparable measurements that we've taken, in which the DE is still saturating at 2100 nm, which is suggested of high efficiency in the mid-IR



Detection efficiency vs I_B and wavelength

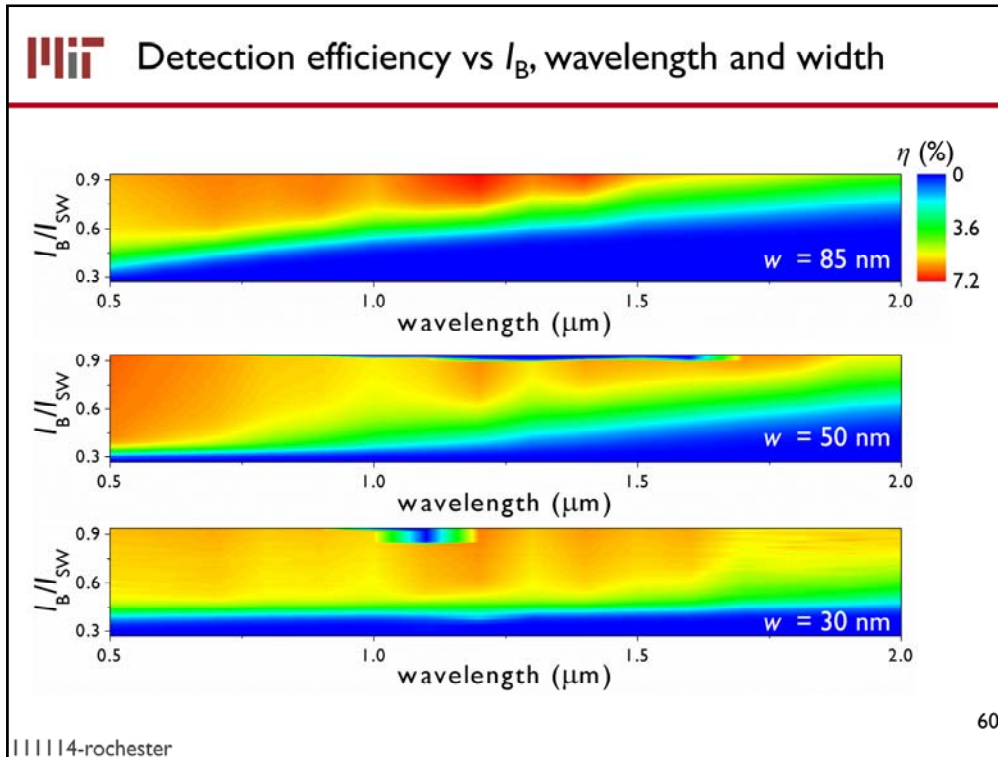


59

111114-rochester

The DE is still saturating at 2100 nm. These results indicate that ultranarrow nanowire SNSPDs would be able to detect longer wavelength photons up to the mid IR

FM6 upgrade dataset for midIR
Francesco Marsili, 9/7/2011



Now let's compare the sensitivity of SNSPDs with different widths.

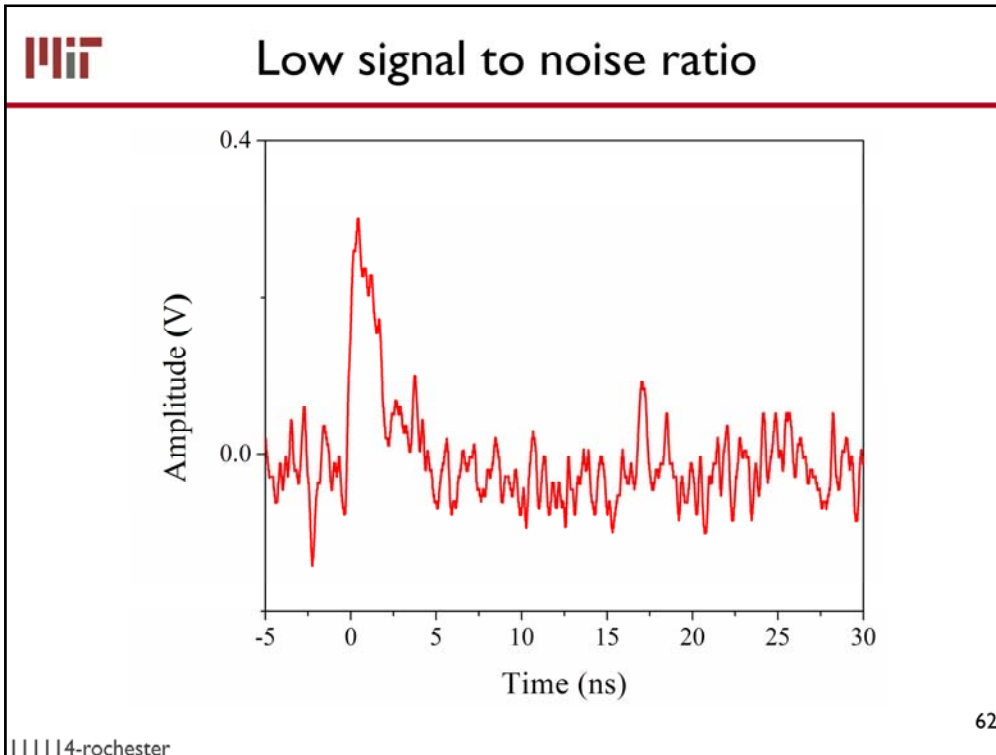
Here I am plotting the detection efficiency vs. bias current, vs. wavelength for SNSPDs based on 30 50 and 85 nm nanowires. As you see the bias range where the DE is flat increases with decreasing w .

Increasing the signal-to-noise ratio

||||4-rochester

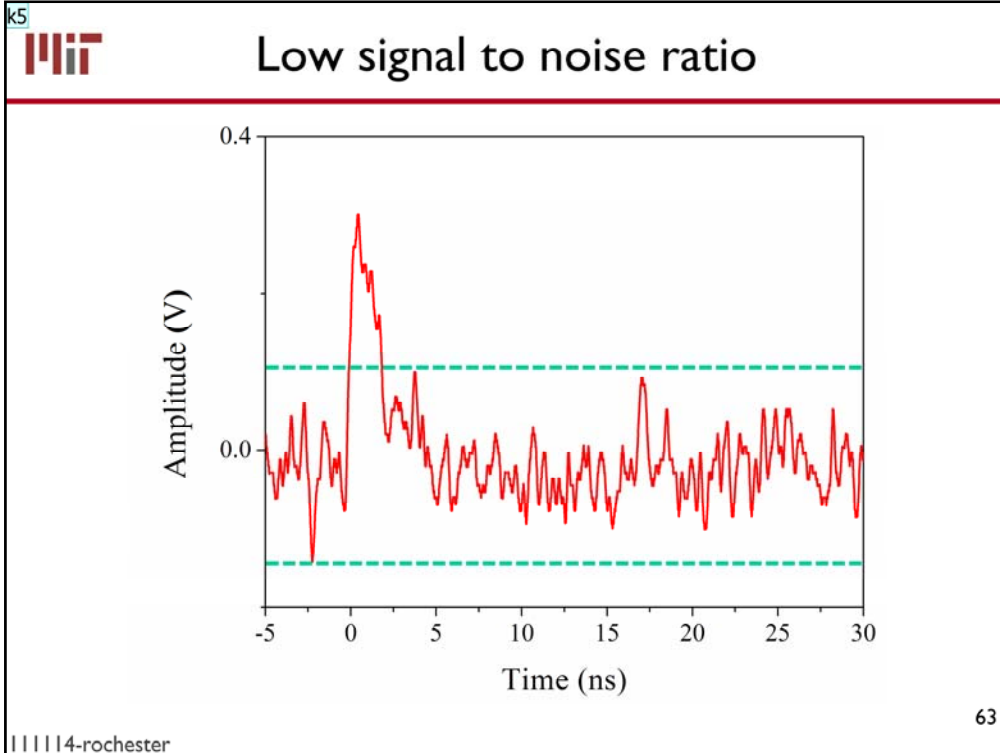
61

Transition slide



The drawback of nanowire SNSPDs is the low SNR. Indeed decreasing the nanowire width of factor 3 or more, I decrease the current pulse from the detectors by the same factor. So the SNSPD signal is much less robust to noise.

This is a single-shot oscilloscope trace of the SNSPD photoresponse.



As you see the signal is of the same order than the peak to peak noise.

Slide 63

k5

20-nm-wide nanowire

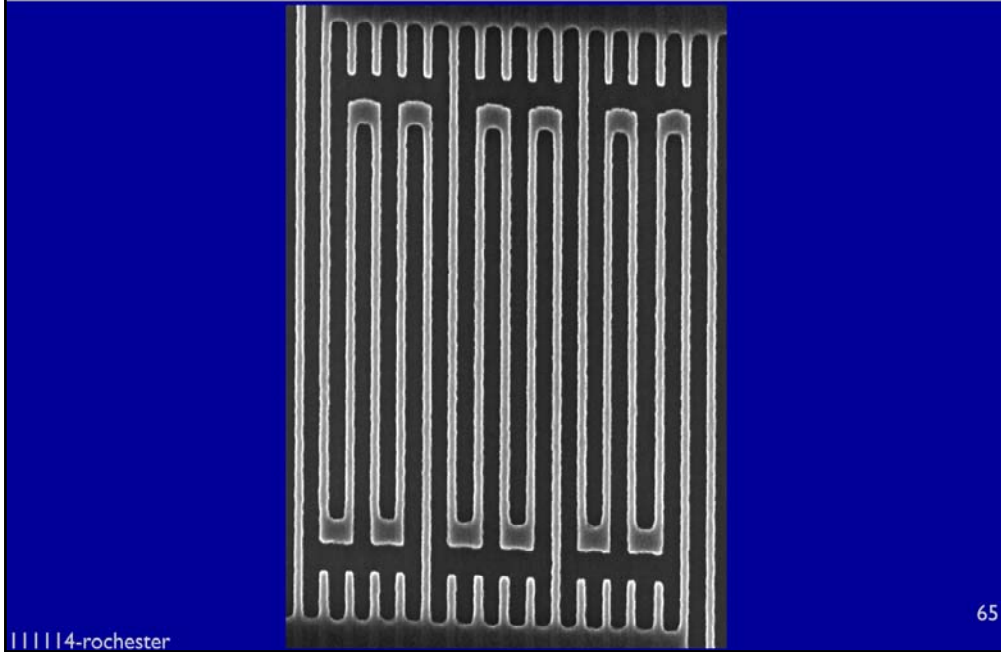
karl, 7/18/2011

“A Cascade Switching Superconducting Single Photon Detector,”

M. Ejrnaes, R. Cristiano, O. Quaranta, S. Pagano, A. Gaggero, F. Mattioli, R. Leoni, B. Voronov, and G. Gol'tsman,

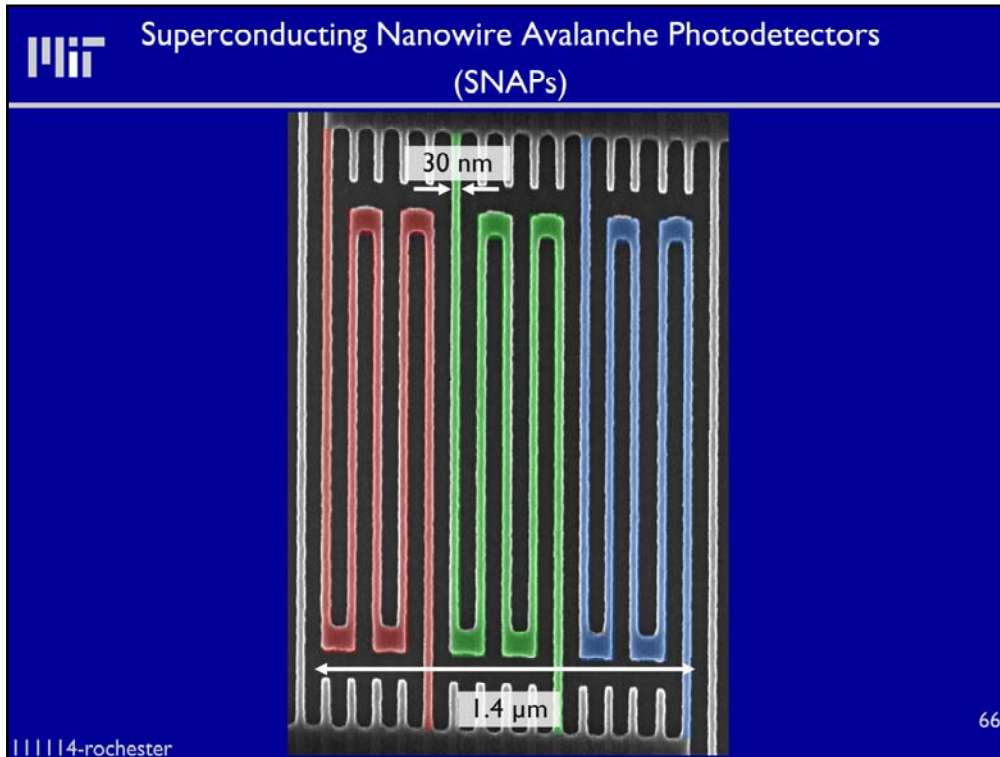
Appl. Phys. Lett. 91, 262509 (2007)

To solve the problem of the low SNR of narrow nanowire SNSPDs, following the ideas of this paper, we designed an avalanche-based device. The device presented here had high SNR, but high jitter. The Superconducting Nanowire Avalanche Photodetector (SNAP).



The structure of SNAPs is the parallel connection of N nanowires.

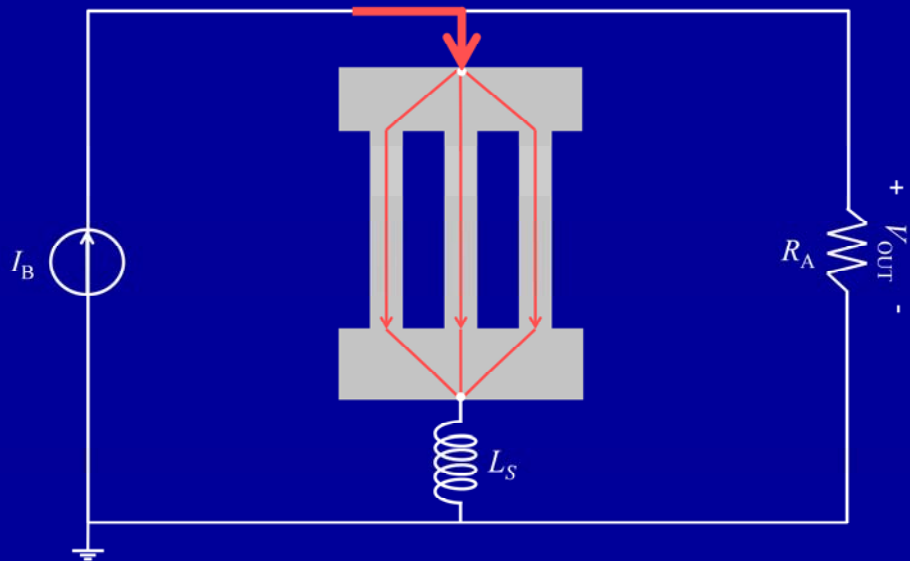
Q33 cssspd
QNN, 4/26/2011



The structure of SNAPs is the parallel connection of N nanowires with detectors colorized



Basic model of SNAP operation



67

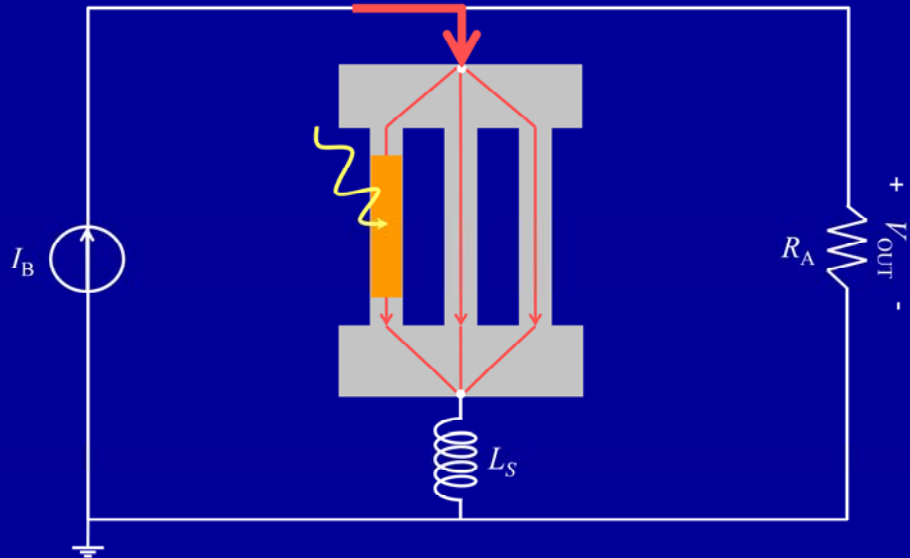
In order to illustrate the SNAP operation mechanism, let's consider this sketch of a 4-SNAP.

The device is biased with a current I_B and it is connected in series with an inductor L_S , whose function is going to be clarified in the following.

Q12



Basic model of SNAP operation



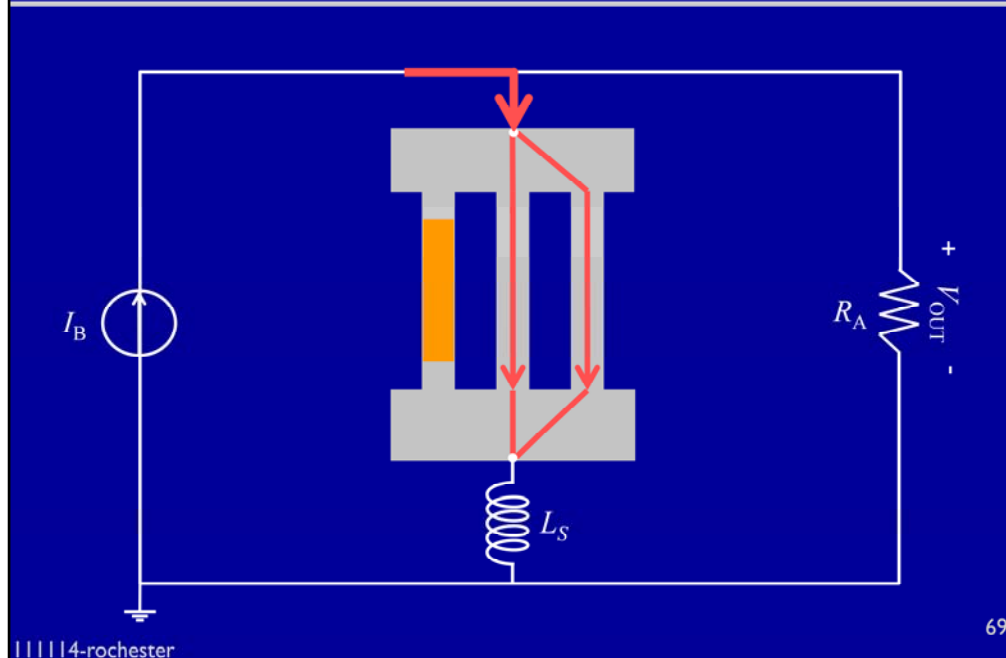
A photon triggers the superconducting-normal transition in one section, which we call initiating.

Slide 68

Q12 wave no thunderbolt
QNN, 4/22/2011

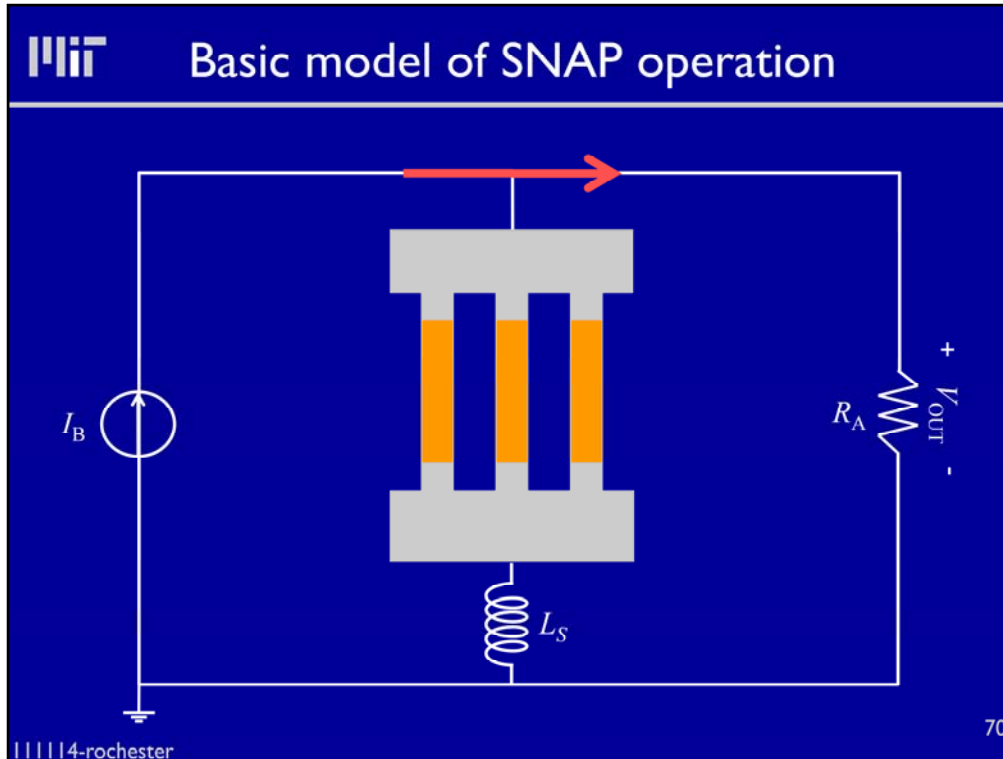


Basic model of SNAP operation



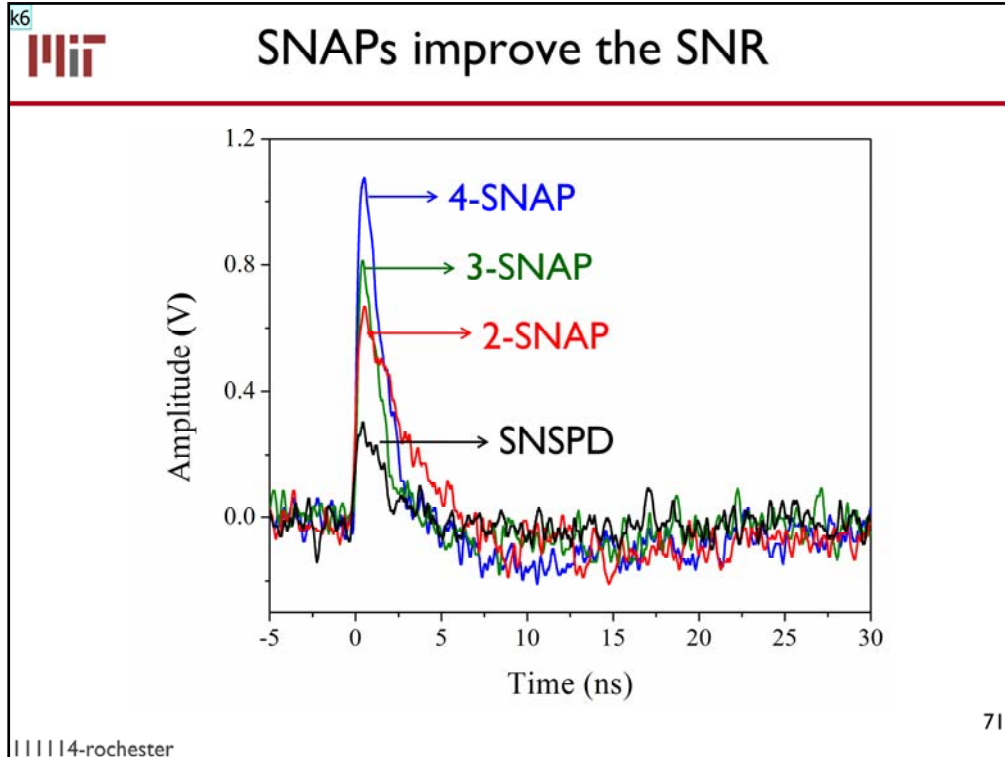
All the current of that section is redistributed between the other 3 sections. The current on each SC section increases by δI . If the series inductor L_S is large enough, no current will leak in the read out.

We call the assumption that all the current through the init section is redistributed only to the secondary sections perfect redistribution.



If the bias current is large enough, the current in the non-firing sections exceeds the critical current (I_C), so they switch to the normal state too.

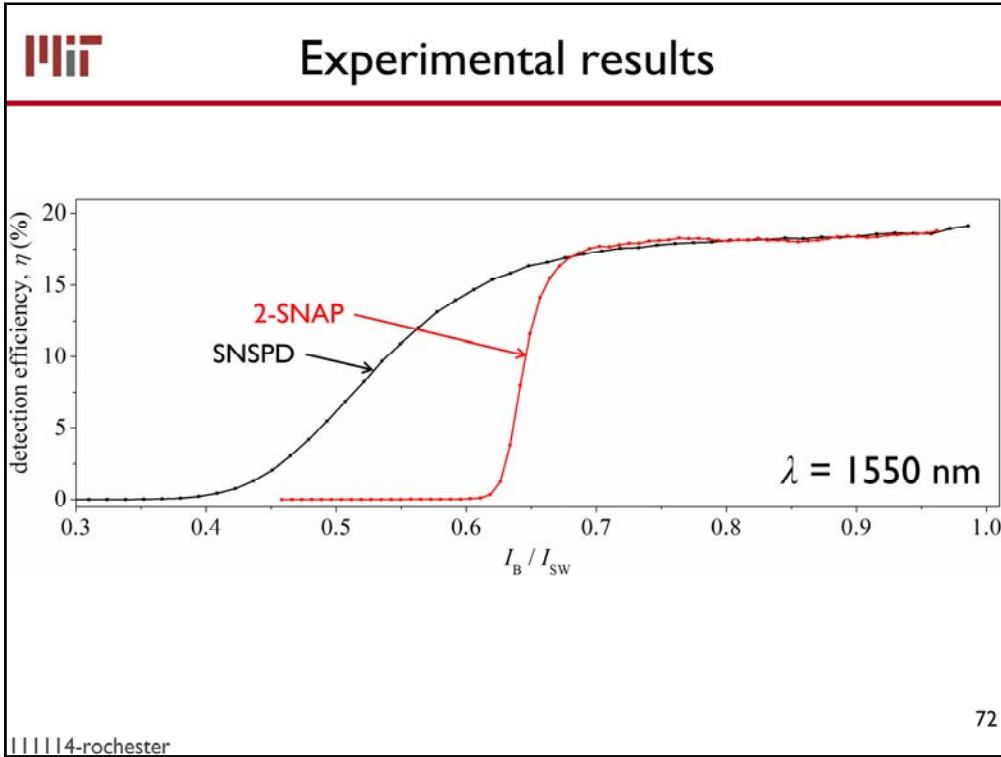
The current through the whole device is then sent to the read out resistance. This current is 4 times higher than the current carried by one section. This amplification effect solves our SNR problem.



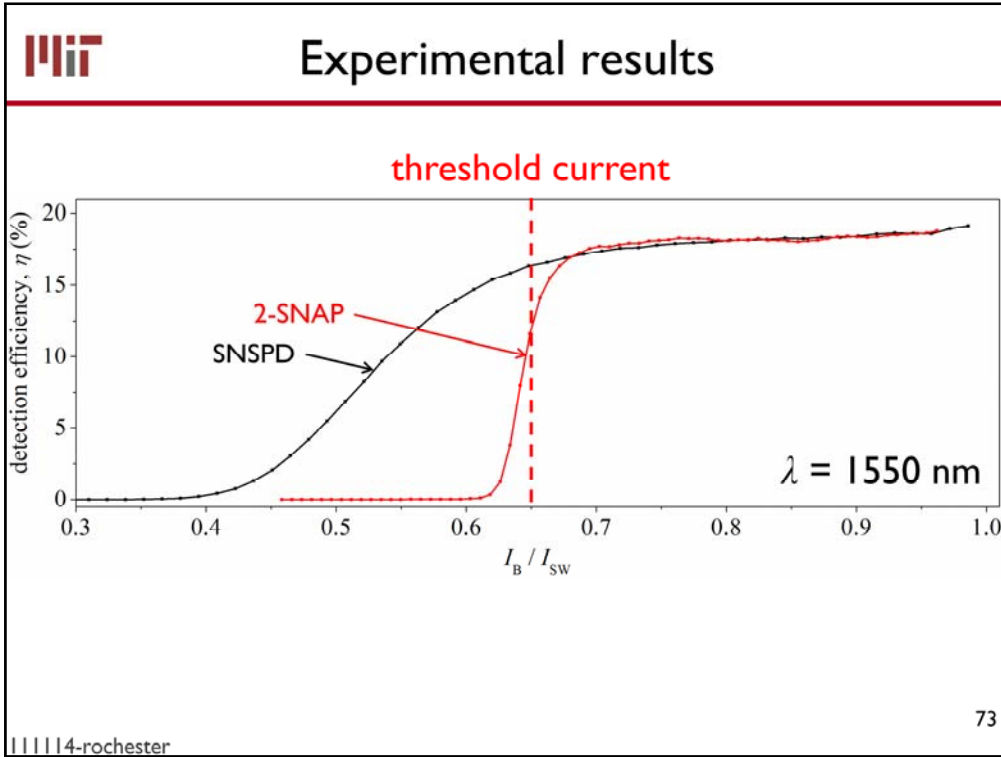
Single-shot oscilloscope trace of the photoresponse pulses of an SNSPD and of a 2-, 3- and 4-SNAP. The nanowires were 20-nm wide. The devices were biased at $0.98I_{SW}$. The signal to noise ratio of a 20-nm-wide-nanowire SNSPD is so low that most of the signal dynamics is within the noise base, so it is not possible to use it as a detector. With SNAPs the situation is largely improved.

Slide 71

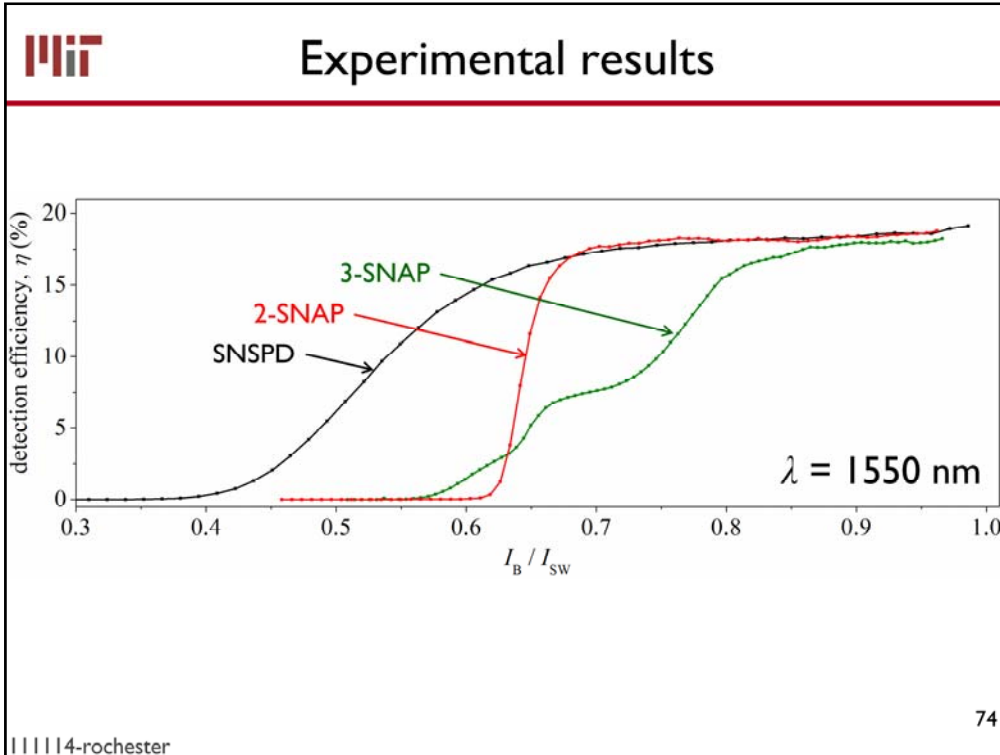
k6 20-nm-wide nanowire
karl, 7/18/2011



Now what does the DE look like?



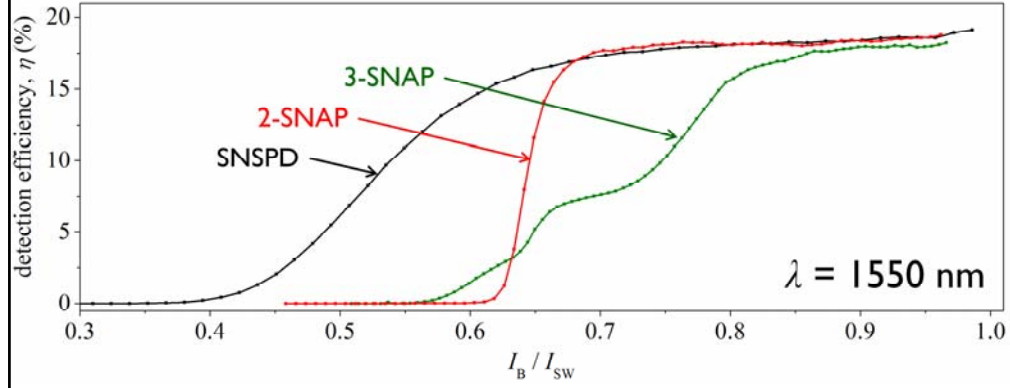
Now what does the DE look like?



Where is the device working as an spd?



Experimental results



In which bias range are 3-SNAPs working as single-photon detectors?

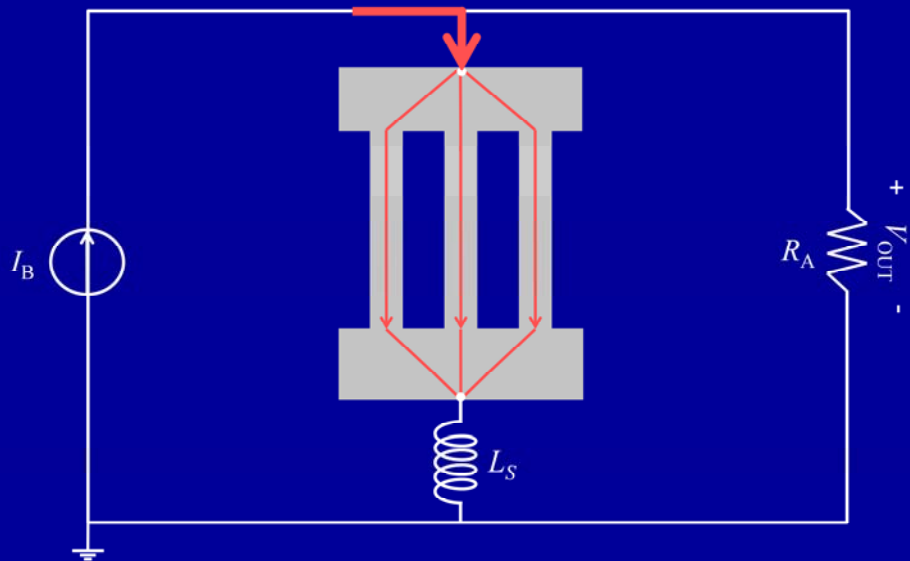
75

111114-rochester

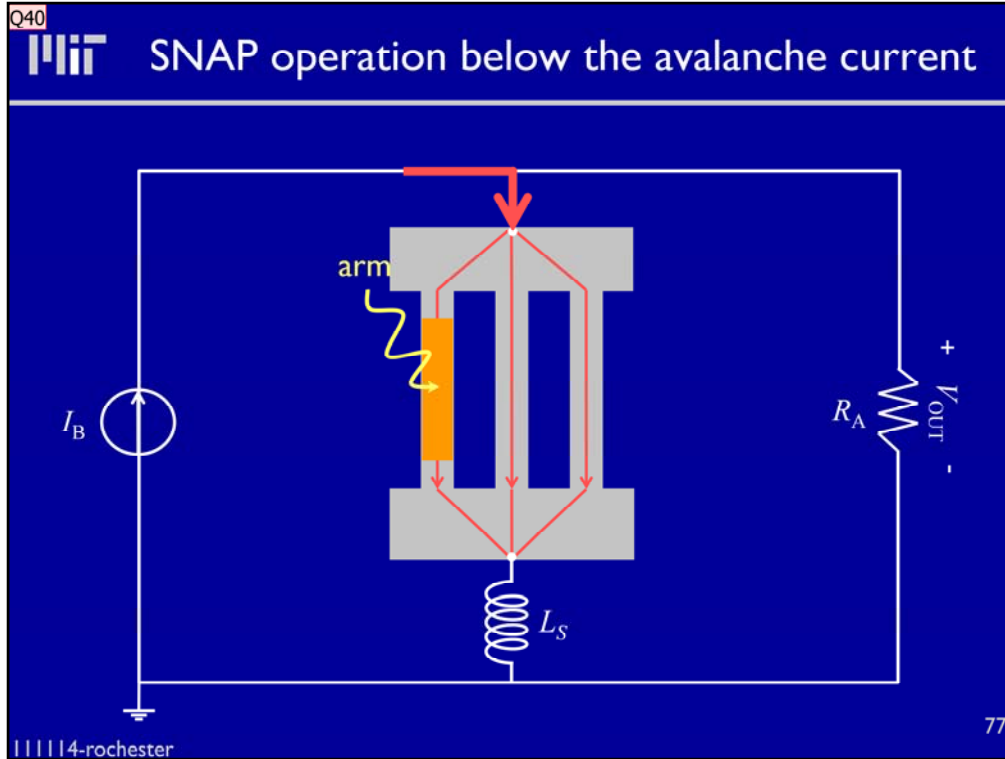
Where is the device working as an spd?



SNAP operation below the avalanche current



In order to answer that question, we modeled the device operation below the minimum bias current necessary to for a photon to trigger an avalanche. Let's see what happens.



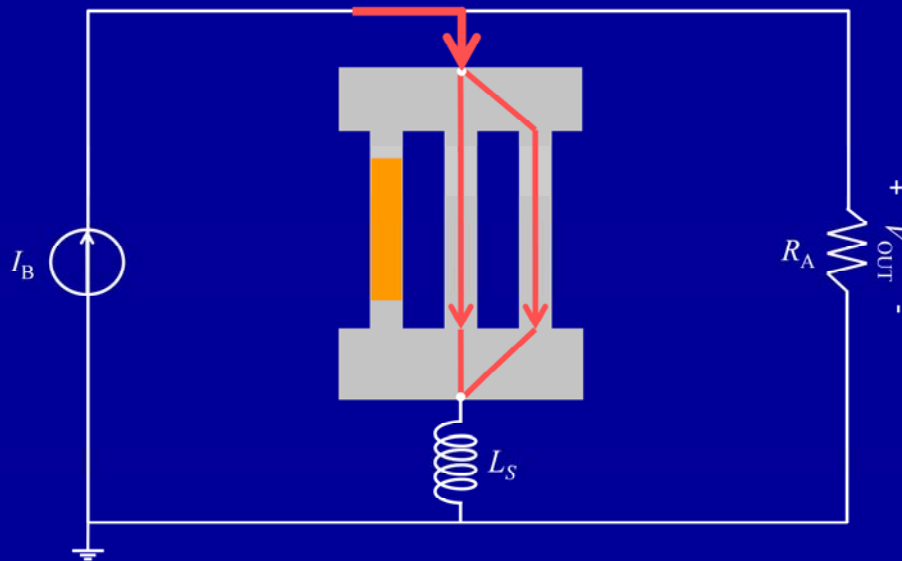
A photon triggers the superconducting-normal transition in one section, which we call initiating.

Slide 77

Q40 wave no thunderbolt
QNN, 4/22/2011



SNAP operation below the avalanche current

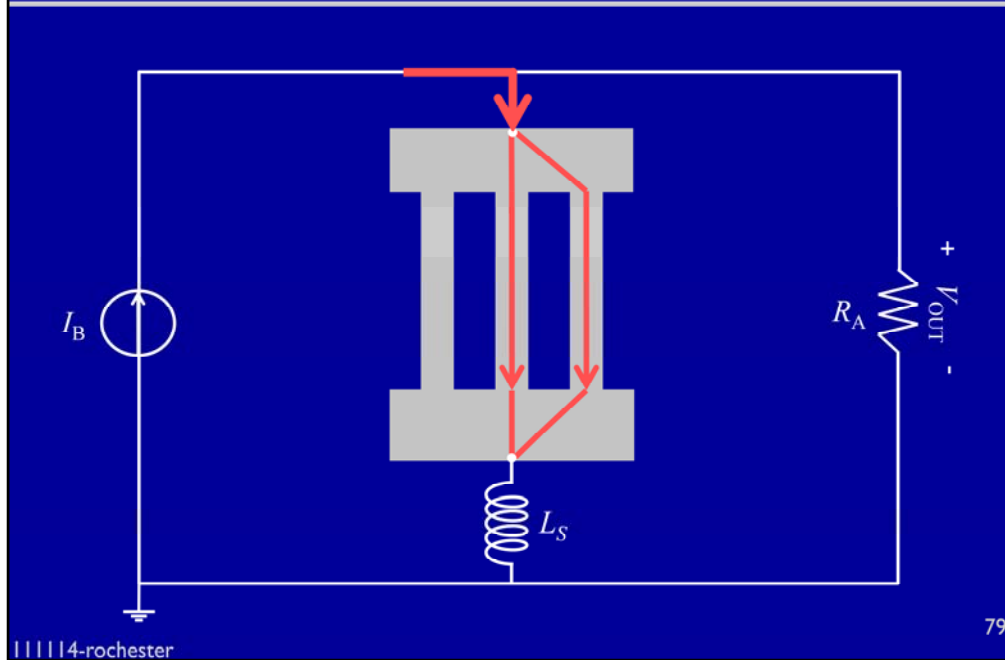


All the current of that section is redistributed between the other 3 sections. The current on each SC section increases by δI . If the series inductor L_S is large enough, no current will leak in the read out.

We call the assumption that all the current through the init section is redistributed only to the sec section perfect redistribution.



SNAP operation below the avalanche current

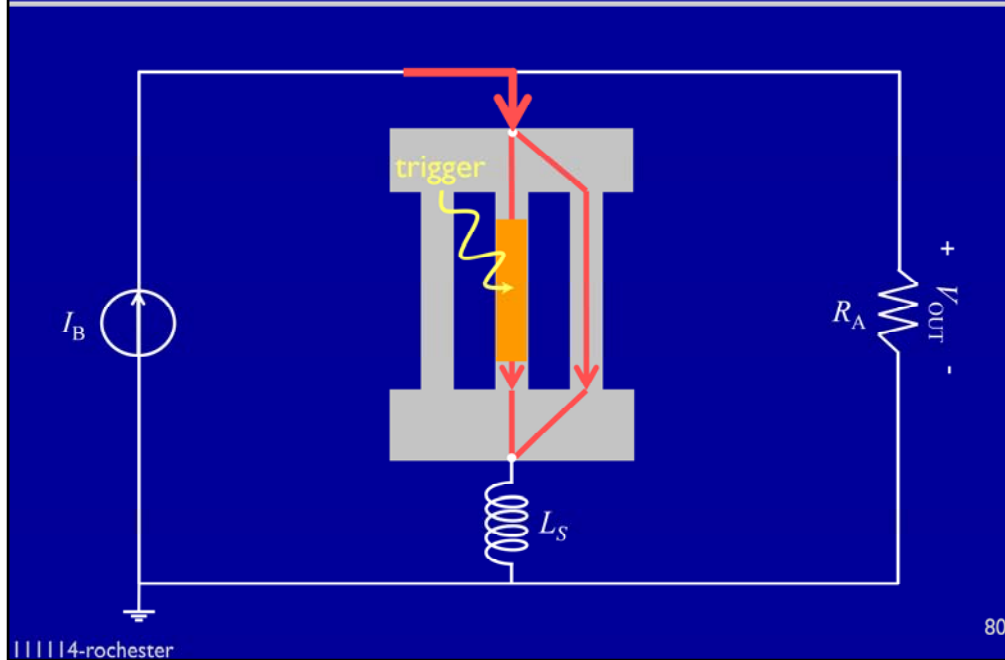


All the current of that section is redistributed between the other 3 sections. The current on each SC section increases by δI . If the series inductor L_S is large enough, no current will leak in the read out.

We call the assumption that all the current through the init section is redistributed only to the sec section perfect redistribution.



SNAP operation below the avalanche current

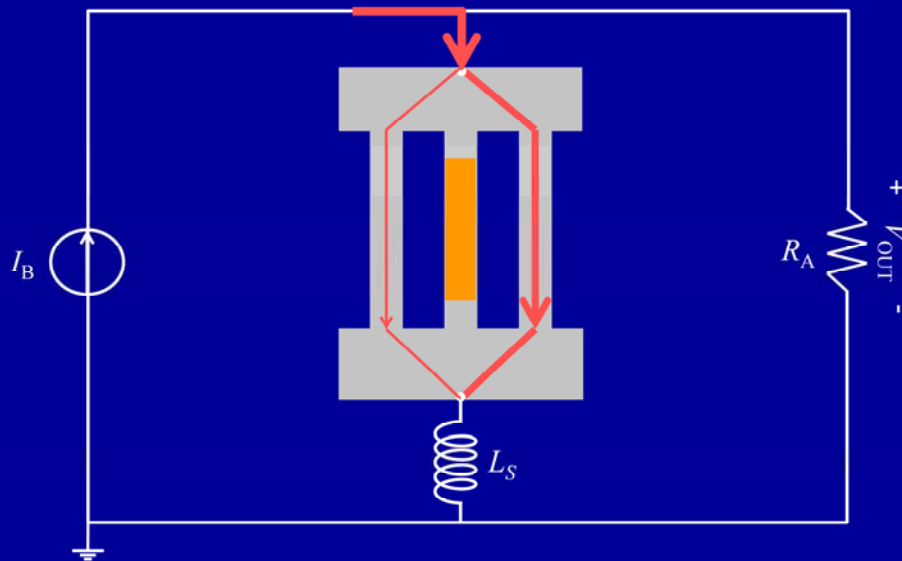


All the current of that section is redistributed between the other 3 sections. The current on each SC section increases by δI . If the series inductor L_S is large enough, no current will leak in the read out.

We call the assumption that all the current through the init section is redistributed only to the sec section perfect redistribution.



SNAP operation below the avalanche current

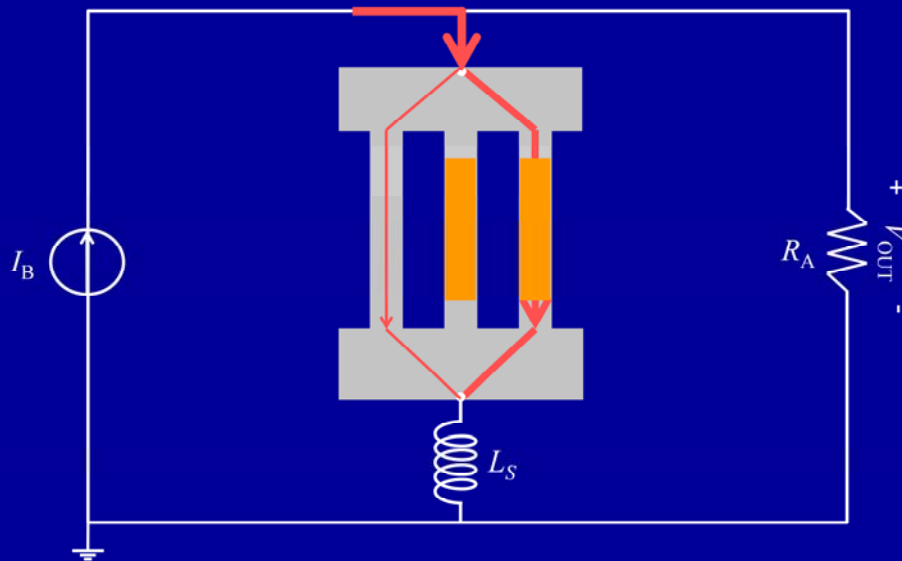


All the current of that section is redistributed between the other 3 sections. The current on each SC section increases by δI . If the series inductor L_S is large enough, no current will leak in the read out.

We call the assumption that all the current through the init section is redistributed only to the sec section perfect redistribution.



SNAP operation below the avalanche current

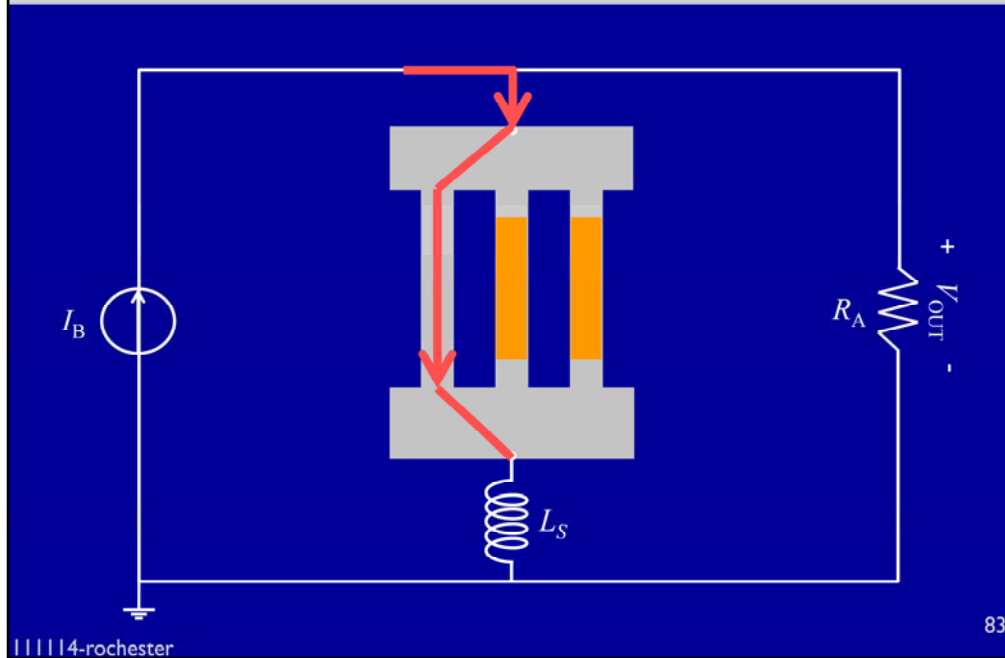


All the current of that section is redistributed between the other 3 sections. The current on each SC section increases by δI . If the series inductor L_S is large enough, no current will leak in the read out.

We call the assumption that all the current through the init section is redistributed only to the sec section perfect redistribution.



SNAP operation below the avalanche current

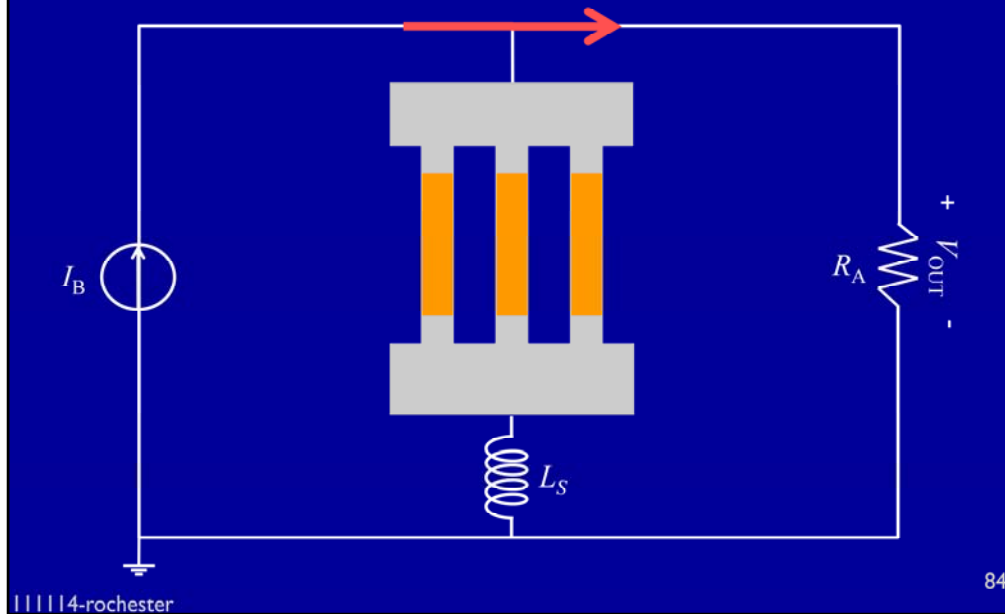


All the current of that section is redistributed between the other 3 sections. The current on each SC section increases by δI . If the series inductor L_S is large enough, no current will leak in the read out.

We call the assumption that all the current through the init section is redistributed only to the sec section perfect redistribution.

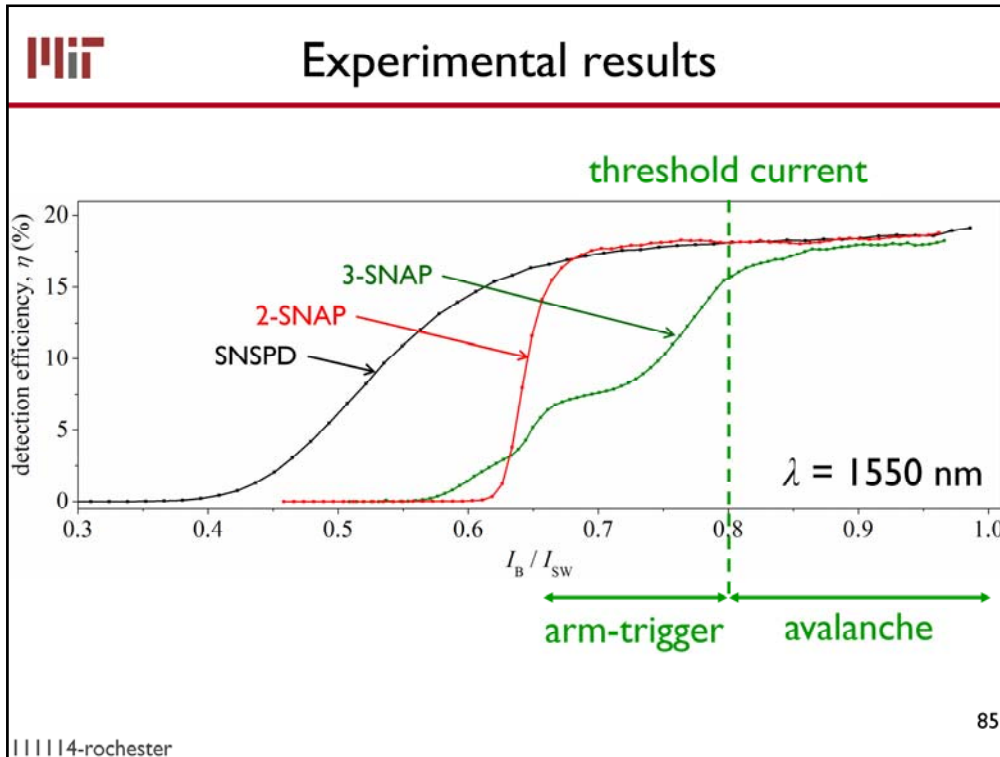


SNAP operation below the avalanche current

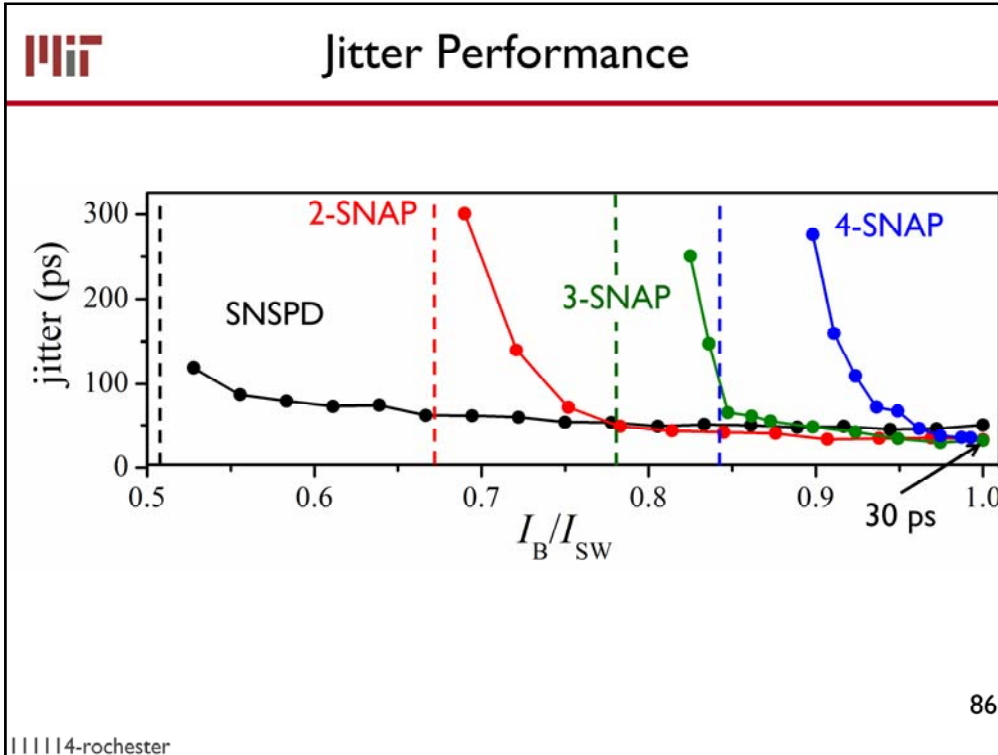


If the bias current is large enough, the current in the non-firing sections exceeds the critical current (I_C), so they switch to the normal state too.

The current through the whole device is then sent to the read out resistance. This current is 4 times higher than the current carried by one section. This amplification effect solves our SNR problem.

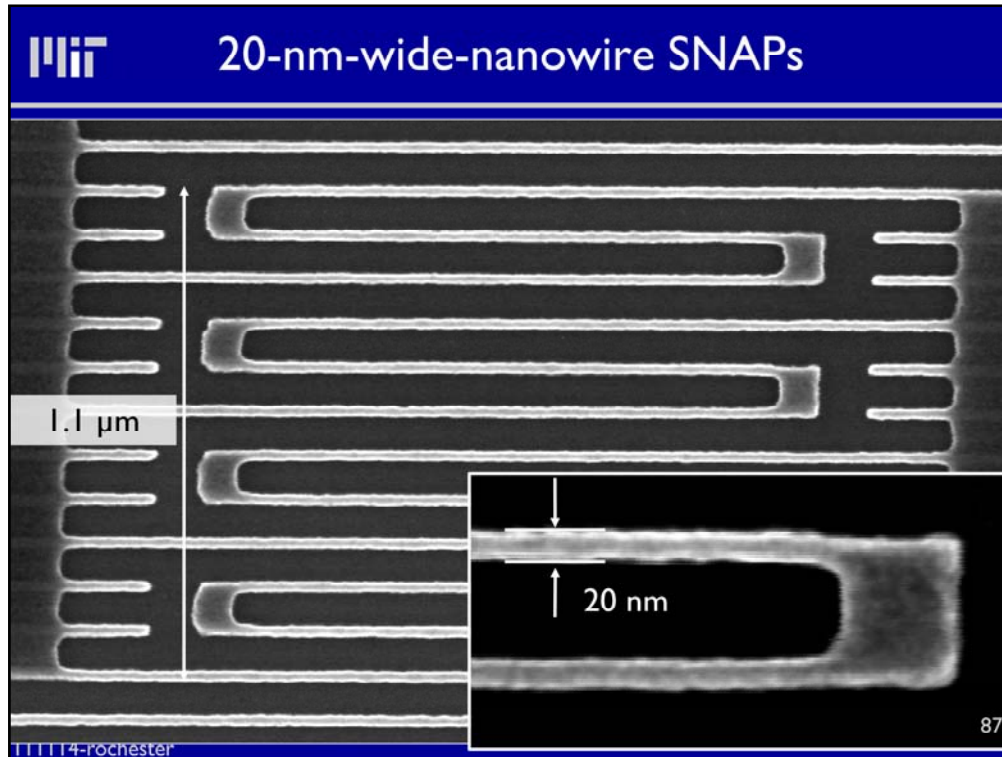


Our experimental results indicate that the min current to have a single ph trigger an avalanche is 80% for a 3-SNAP. Above that current the device works as an SPD, while below it works in arm-trigger regime.



We measured the jitter of sspds and snaps vs the bias current and found that the devices have a jitter of 30 ps at high bias close to ISW. The jitter rapidly increases when the SNAPs reach the avalanche threshold current and the SNSPD the cut off current.

This graph and the DE tell you what is the bias range in which you want to use the devices to have single photon detection with high time resolution.

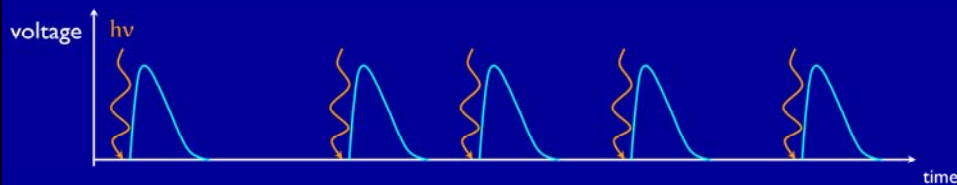


These convinced us that the SNAPs could be used to improve the SNR of our det. Scanning electron microscope (SEM) images of hydrogen silsesquioxane (HSQ) nanowires on a 4-nm-thick NbN film. The nanowires are 20-nm wide and are arranged in a meander pattern with 100-nm pitch. This structures was obtained by electron beam lithography (30 kV acceleration voltage) on 45-nm-thick HSQ.



Inter-arrival time measurements

Avalanche mode:



|||||4-rochester

88

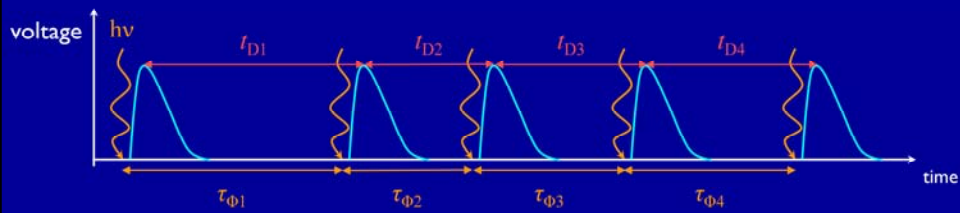
The experimental results shown previously can be qualitatively explained with our model. To prove the validity of our model quantitatively we measured the photoresponse pulse inter-arrival time.

Here you see a sketch of our model of the SNAP operation in avalanche regime. Each time a photon is detected, it triggers an avalanche, hence a pulse.



Inter-arrival time measurements

Avalanche mode:



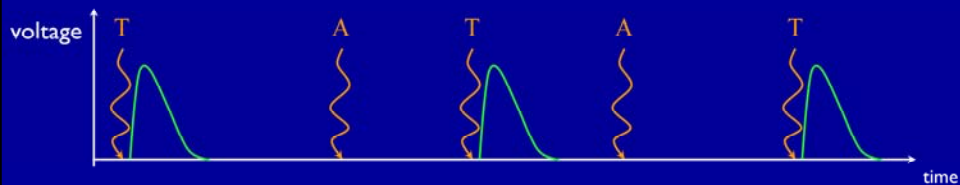
$$f_{t_D}(t) = f_{\tau_{\phi}}(t)$$

As each time a photon is detected, it triggers a pulse, t_D equals the detected photon inter-arrival time τ_{ϕ} .



Inter-arrival time measurements

Arm-trigger mode:



|||||4-rochester

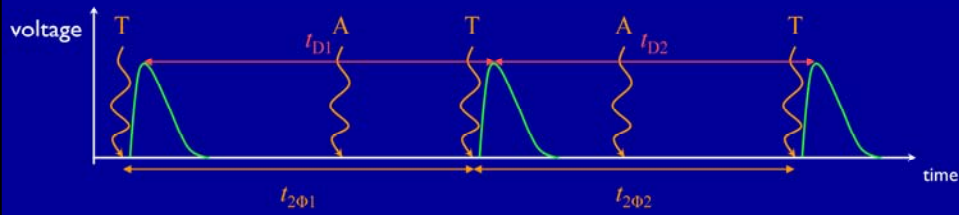
90

Here you see a sketch of the model of the SNAP operation in A-T regime. Now an avalanche is triggered by the detection of two subsequent photons.



Inter-arrival time measurements

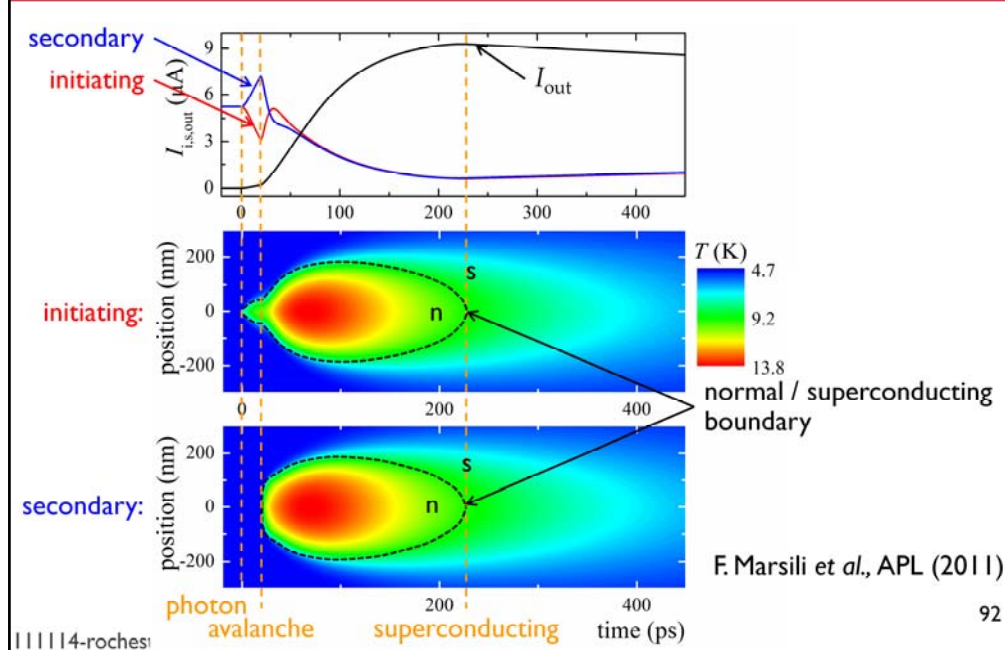
Arm-trigger mode:



$$f_{t_D}(t) = f_{\tau_{2\phi}}(t)$$

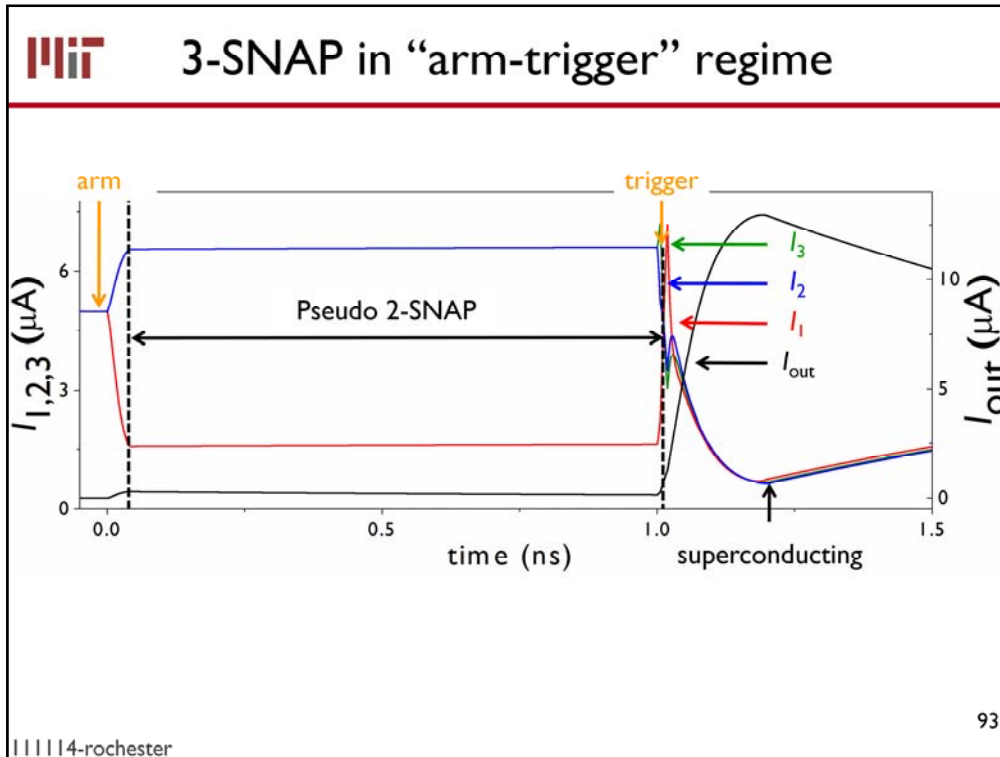
So in this case t_D equals the two-detected-photon inter-arrival time $\tau_{2\phi}$.

MIT Electro-thermal simulation of SNAPs



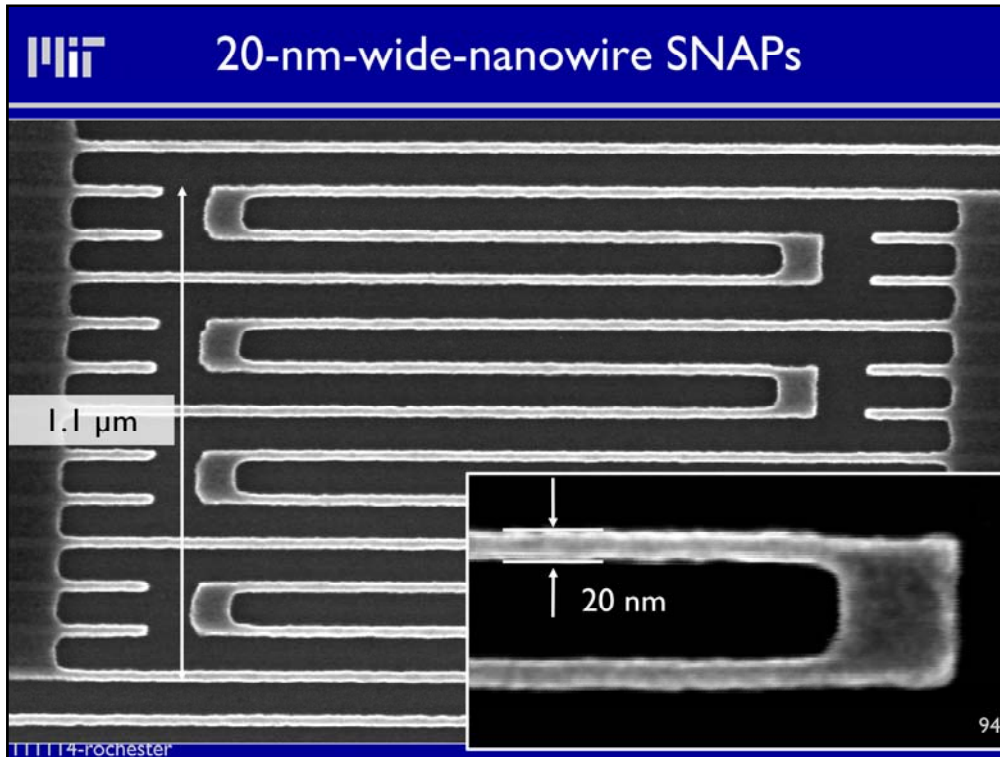
“low” bias condition

As the bias current is too low, the current redistribution in the non-firing sections is not sufficient to make them switch. Therefore no avalanche is triggered. All a ph does is redistributing the bias current among the sections. Repeating the simulation for several bias conditions, we can find IAV.



Here is our model of dev operation in the low-bias regime.

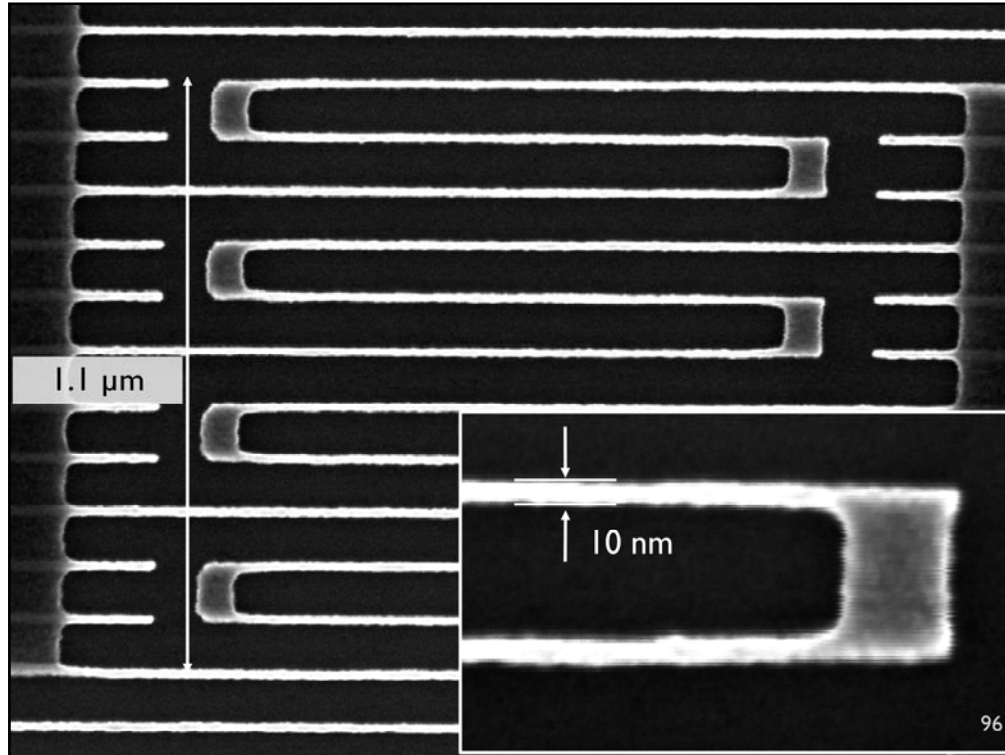
We ran another E-T simulation with a 3-SNAP. The bias current is $<I_{AV}$, but this time we send 2 subsequent photons on two different sections. The 1st photon (arm photon) redistributes the currents in the sections, so the firing section becomes unbiased and the others are biased very close to ISW.



These convinced us that the SNAPs could be used to improve the SNR of our det. Scanning electron microscope (SEM) images of hydrogen silsesquioxane (HSQ) nanowires on a 4-nm-thick NbN film. The nanowires are 20-nm wide and are arranged in a meander pattern with 100-nm pitch. This structures was obtained by electron beam lithography (30 kV acceleration voltage) on 45-nm-thick HSQ.

- Scaling sensitivity out to longer wavelengths
 - (is high-efficiency single-photon detection possible at 10 μm ?)
- Understanding the source of jitter
 - Intrinsic to material? Electronic? Thermal? Electro-thermal?
 - Dependent on design/architecture? Engineerable?
- Can we break the 1 ns speed limit?
 - Need to investigate new materials
 - Need to investigate new device designs

These are some thoughts on what the future may bring.



Scanning electron microscope (SEM) images of hydrogen silsesquioxane (HSQ) nanowires on a 4-nm-thick NbN film. The nanowires are 10-nm wide and are arranged in a meander pattern with 100-nm pitch. This structures was obtained by electron beam lithography (30 kV acceleration voltage) on 45-nm-thick HSQ. Characterization is still in progress.

Acknowledgements

MIT Quantum Nanostructures and Nanofabrication Group

Vikas Anant (now graduated)
Francesco Bellei
Eric Dauler (Lincoln Lab Fellow, now at
Lincoln Laboratory)
Charles Herder (undergraduate)
Xiaolong Hu
Francesco Marsilli (post-doc, now at
NIST)
Faraz Najafi
Joel Yang (ASTAR Fellowship)

MIT Lincoln Laboratory

Andrew J. Kerman
Richard Molnar
Bryan Robinson
Scott Hamilton

NIST

Martin J. Stevens
Burm Baek
Sae Woo Nam
Richard P. Mirin

Other Collaborators

M. Csete (U. of Szeged)
Boris Voronov (MSPU)
Gregory Gol'tsman (MSPU)

Sponsors

AFOSR, IARPA, DARPA, NASA, NSF

11114-rochester

People who have made contributions to the various results presented.

END OF
PRESENTATION

Transition slide